

# A three Higgs doublet model with symmetry-suppressed flavour changing neutral currents

Dipankar Das<sup>a,\*</sup>, P.M. Ferreira<sup>b,c,†</sup>, António Morais<sup>d,‡</sup>, Ian Padilla-Gay<sup>e,§</sup>, Roman Pasechnik<sup>f,¶</sup>

<sup>a</sup>*Indian Institute of Technology, Khandwa Road, Simrol, Indore 453 552, India*

<sup>b</sup>*Instituto Superior de Engenharia de Lisboa — ISEL, 1959-007 Lisboa, Portugal*

<sup>c</sup>*Centro de Física Teórica e Computacional, Faculdade de Ciências,  
Universidade de Lisboa, Campo Grande, 1749-016 Lisboa, Portugal*

<sup>d</sup>*Departamento de Física da Universidade de Aveiro and  
Centre for Research and Development in Mathematics and Applications (CIDMA)*

*Campus de Santiago, 3810-183 Aveiro, Portugal*

<sup>e</sup>*Niels Bohr International Academy and DARK, Niels Bohr Institute,  
University of Copenhagen, Blegdamsvej 17, 2100, Copenhagen, Denmark*

<sup>f</sup>*Department of Astronomy and Theoretical Physics, Lund University, Sölvegatan 14A, 223 62 Lund, Sweden*

## Abstract

We construct a three-Higgs doublet model with a flavour non-universal  $U(1) \times Z_2$  symmetry. That symmetry induces suppressed flavour-changing interactions mediated by neutral scalars. New scalars with masses below the TeV scale can still successfully negotiate the constraints arising from flavour data. Such a model can thus encourage direct searches for extra Higgs bosons in the future collider experiments, and includes a non-trivial flavour structure.

## 1 Introduction

The properties of the new resonance observed at the LHC in 2012 [1, 2] seem tantalizingly close to those of the Higgs boson predicted by the Standard Model (SM) (for instance, see [3, 4]). The particle spectrum predicted by the SM has now been fully confirmed, but many important questions in particle physics are left unanswered: the smallness of neutrino masses, the fermion mass hierarchy, the colossal asymmetry between the quantity of matter and antimatter in the universe and the nature of dark matter are a few of such unresolved issues. They are usually taken as hints for the existence of new physics (NP) beyond the SM (BSM). RP: Typical BSM scenarios that aim to fix one or more such shortcomings of the SM often end up extending the scalar sector of the SM. In these extensions, the 125 GeV scalar observed at the LHC is not the only scalar in the spectrum but the first one in a series of others to follow. This is an intriguing possibility which motivates us for a closer inspection of the properties of the observed scalar and inspires us to carry on our efforts to look for new resonances at the collider experiments.

When it comes to extending the scalar sector of the SM, adding replicas of the SM Higgs-doublet is one of the simplest ways to do it. Such extensions do not alter the tree level value of the electroweak (EW)  $\rho$ -parameter. Two Higgs-doublet models (2HDMs), which add only one extra doublet to the SM Higgs sector, have received its fair share of attention through the years. They were proposed by T.D. Lee in 1973 [5] as a means to obtain a spontaneous breaking of the CP symmetry, and boast a rich phenomenology. Other than the possibility of spontaneous CP breaking, RP: such models contain a richer particle spectrum, with a charged scalar and a total

---

\*[d.das@iiti.ac.in](mailto:d.das@iiti.ac.in)

†[pedro.ferreira@fc.ul.pt](mailto:pedro.ferreira@fc.ul.pt)

‡[aapmorais@ua.pt](mailto:aapmorais@ua.pt)

§[ian.padilla@nbi.ku.dk](mailto:ian.padilla@nbi.ku.dk)

¶[roman.pasechnik@hep.lu.se](mailto:roman.pasechnik@hep.lu.se)

of three neutral ones, RP: may feature dark matter candidates in certain scenarios, and RP: generically give rise to the tree-level scalar-mediated flavour changing neutral currents (FCNCs). RP: Indeed, one ominous outcome of adding extra scalar doublets is that the fermions of a particular charge will now receive their masses from multiple Yukawa matrices and consequently, diagonalization of their mass matrices will no longer guarantee the simultaneous diagonalization of the Yukawa matrices. Therefore, in general, there will exist FCNCs at tree-level mediated by neutral scalars.

Experimental data from the flavour sector – to wit, neutral meson mass differences for Kaons and B-mesons, or  $\epsilon_K$  data – strongly constrain such FCNCs, typically forcing the extra scalars to have masses above 1 TeV [6]. An alternative is to fine-tune the FCNC interactions so that they are very small, though for some models cancellations between CP-even and CP-odd contributions to the amplitudes off the observables mentioned allow for below-TeV scalars with a minimal fine-tuning (see, for instance, [7–9]). Another possibility is to assume *alignment* between different Yukawa matrices [10–12], though that is an *ansatz* which is not preserved under renormalization [13]. There is yet another possibility, however: the BGL (Branco-Grimus-Lavoura) model [14, 15] is a remarkable version of the 2HDM wherein FCNC interactions are *naturally* small – this results from the imposition of a flavour-violating symmetry, *i.e.* a symmetry which treats some generations of fermions differently from others. As a consequence of this symmetry, FCNC couplings are suppressed by off-diagonal Cabibbo-Kobayashi-Maskawa (CKM) matrix elements. The phenomenology of the model has been studied quite thoroughly (see, for instance, [16, 17]) and it remains a valid and exciting possibility for BSM physics.

As a next-to-minimal possibility along these lines, recent years have seen a growing interest in the topic of three Higgs-doublet models (3HDMs). These models add two extra scalar doublets on top of the SM one, thereby conforming to the aesthetic appeal of having three scalar generations in harmony with the three generations of fermions. An early proposal by Weinberg [18] included two discrete symmetries which yielded flavour conservation. A recent study [19], following earlier work in [20–22], used a generalized CP symmetry (called CP4) to constrain the vast parameter space of 3HDM, and was found to have large regions of parameter space which conformed with experimental constraints in the flavour RP: and scalar sectors. That model, however, used the liberty in parameters present in the Yukawa sector to fit all observables, but the FCNC couplings were not necessarily small.

In this article, we will attempt to implement the BGL method in a 3HDM framework. We construct a 3HDM with a  $U(1) \times Z_2$  flavor symmetry, where we also achieve the smallness of the FCNC couplings in a way similar to the BGL case. As a result, we find that relatively light scalars within the reach of the current and future collider experiments, can successfully pass through the stringent constraints arising from the flavor data. To motivate future searches, we also outline the possible signatures of the nonstandard scalars present in our model.

Our article is organized as follows. In section 2 we review the framework of BGL models. Then, in section 3, we will build our model, a 3HDM endowed with a  $U(1) \times Z_2$  symmetry with a non-trivial structure in the Yukawa sector. In section 4 we review the constraints imposed upon the model, both theoretical – boundedness from below, unitarity, electroweak precision bounds – and experimental – LHC Higgs data and searches for heavier scalars, flavour physics data, among others. In section 5 we explain in detail the procedure we followed to perform a thorough numerical scan of the model and present the results we found for the parameter space that survives all constraints imposed upon the model. We conclude in section 6 with an overview of this work and a discussion of its RP: significance.

## 2 The BGL model

The BGL model is a version of the 2HDM where the scalar interactions with fermions violate flavour – meaning, unlike the interactions of the photon and  $Z$  boson, the neutral scalars in the BGL model “jump families” like the  $W$  boson does. In the more usual versions of the 2HDM the existence of FCNC in the scalar sector is avoided by imposing a  $Z_2$  [23, 24] or  $U(1)$  [25] symmetry on the model, which forces each fermion of the same charge to couple to a single doublet, thereby preventing FCNC. The reason for doing this in the first place is

the fact that tree-level mediated FCNC would make significant contributions to flavour sector observables such as the mass differences of the  $K^0$ ,  $B_d$  or  $B_s$  mesons, or to the  $\epsilon_K$  quantity, ruining an agreement found within the SM for those quantities – unless the masses of the new scalars are all of order TeV, or the FCNC Yukawa couplings are tuned to be very small.

The BGL model is remarkable since it forces the FCNC couplings to be heavily suppressed as the result of a symmetry. The model therefore provides a simple and natural explanation as to why NP contributions to flavour observables would not ruin the agreement found within the SM, without the need of any fine-tuning. To understand how this is achieved, consider the Yukawa Lagrangian for the quark sector in the 2HDM,

$$-\mathcal{L}_Y = \sum_{a,b=1}^3 \left\{ \bar{Q}_L^a [(\Gamma_1)_{ab} \phi_1 + (\Gamma_2)_{ab} \phi_2] n_R^b + \bar{Q}_L^a [(\Delta_1)_{ab} \tilde{\phi}_1 + (\Delta_2)_{ab} \tilde{\phi}_2] p_R^b \right\} + \text{h.c.}, \quad (1)$$

where  $Q_L^a = (p_L^a n_L^a)^T$  and  $\phi_i$  RP: are the SU(2) weak isospin (left-handed) quark and Higgs doublets, respectively, and  $\tilde{\phi}_k = i\sigma_2 \phi_k^*$ . The  $p$  and  $n$  fields are the positively and negatively charged quark fields, respectively. Upon rotation to the mass basis they will yield the physical up and down quarks. The  $a$  and  $b$  are fermion family indices.  $\Gamma$  and  $\Delta$  are  $3 \times 3$  Yukawa coupling matrices for the down and up sector, respectively. Upon spontaneous symmetry breaking, the scalar doublets develop neutral vacuum expectation values (VEVs), such that<sup>1</sup>  $\langle \phi_1 \rangle = v_1/\sqrt{2}$  and  $\langle \phi_2 \rangle = v_2/\sqrt{2}$ , with  $v_1^2 + v_2^2 = (246 \text{ GeV})^2$ . We define  $\tan \beta = v_2/v_1$ . For a CP-conserving model (both at the explicit and vacuum levels), the model will have a charged scalar  $H^+$ , a pseudoscalar  $A$  and two CP-even scalars,  $h$  and  $H$ . The  $2 \times 2$  CP-even mass matrix is diagonalized via an angle  $\alpha$ .

The up and down quark mass matrices are then given by

$$M_p = \frac{1}{\sqrt{2}} (\Delta_1 v_1 + \Delta_2 v_2) , \quad M_n = \frac{1}{\sqrt{2}} (\Gamma_1 v_1 + \Gamma_2 v_2) , \quad (2)$$

the eigenvalues of which will be the physical quark masses. In fact, these mass matrices will be bidiagonalized in the usual form as

$$D_u = V_L^\dagger M_p V_R = \text{diag}\{m_u, m_c, m_t\} , \quad D_d = U_L^\dagger M_n U_R = \text{diag}\{m_d, m_s, m_b\} , \quad (3)$$

where  $m_x$  are the physical quark masses, and  $V$  and  $U$  are U(3) matrices. These matrices relate the physical quark states  $u$  and  $d$  to the  $p$  and  $n$  original states in the following manner:

$$\begin{aligned} p_L &= V_L u_L , & p_R &= V_R u_R , \\ n_L &= U_L d_L , & n_R &= V_R d_R . \end{aligned} \quad (4)$$

The CKM matrix is then obtained as

$$V = V_L^\dagger U_L . \quad (5)$$

We also define the following matrices,

$$N_u = \frac{1}{\sqrt{2}} V_L^\dagger (\Delta_1 v_2 - \Delta_2 v_1) V_R , \quad N_d = \frac{1}{\sqrt{2}} U_L^\dagger (\Gamma_1 v_2 - \Gamma_2 v_1) U_R , \quad (6)$$

which end up being related to the Yukawa couplings between the physical scalars and quarks. In fact, with the usual conventions (see for instance [9, 26]), the Yukawa Lagrangian for the physical fields may be written as

$$\begin{aligned} -\mathcal{L}_Y &= \frac{iA}{v} \left[ \bar{u} (N_u P_R - N_u^\dagger P_L) u + \bar{d} (N_d^\dagger P_L - N_d P_R) d \right] \\ &\quad + \frac{h}{v} \bar{u} [(s_{\beta-\alpha} M_u - c_{\beta-\alpha} N_u^\dagger) P_L + (s_{\beta-\alpha} M_u - c_{\beta-\alpha} N_u) P_R] u \end{aligned}$$

---

<sup>1</sup>We are assuming these VEVs are real which is the case of the BGL model but the generalization to complex ones is trivial.

$$\begin{aligned}
& + \frac{h}{v} \bar{d} \left[ (s_{\beta-\alpha} M_d - c_{\beta-\alpha} N_d^\dagger) P_L + (s_{\beta-\alpha} M_d - c_{\beta-\alpha} N_d) P_R \right] d \\
& + \frac{H}{v} \bar{u} \left[ (c_{\beta-\alpha} M_u + s_{\beta-\alpha} N_u^\dagger) P_L + (c_{\beta-\alpha} M_u + s_{\beta-\alpha} N_u) P_R \right] u \\
& + \frac{H}{v} \bar{d} \left[ (c_{\beta-\alpha} M_d + s_{\beta-\alpha} N_d^\dagger) P_L + (c_{\beta-\alpha} M_d + s_{\beta-\alpha} N_d) P_R \right] d \\
& + \frac{\sqrt{2}H^+}{v} \bar{u} (N_u^\dagger V P_L - V N_d P_R) d + \frac{\sqrt{2}H^-}{v} \bar{d} (V^\dagger N_u P_R - N_d^\dagger V^\dagger P_L) u,
\end{aligned} \tag{7}$$

where we used the notation  $s_x \equiv \sin x$ ,  $c_x \equiv \cos x$ . On a side note, we can see from the above Lagrangian how in the *alignment limit* the lighter Higgs' Yukawa interactions are exactly like those of the SM particles: in that limit one has  $\sin(\beta - \alpha) = 1$  – which forces the vertices between  $h$  and the electroweak gauge bosons to be identical to those of the SM Higgs particle – and therefore the Yukawa couplings of  $h$  to quark pairs are proportional to the quark mass, since the contribution of the  $N$  matrices vanishes.

In models with flavour conservation, each family of fermions of the same electric charge couples to a single **RP: Higgs** doublet, via the imposition of discrete  $Z_2$  [23,24] or global U(1) [25] symmetries. Then, the diagonalization of the  $M_u$  and  $M_d$  matrices, eq. (3) is the same as that of matrices  $N_u$  and  $N_d$  and there are no flavour-violating Yukawa interactions mediated by neutral scalars. In general, though, that will not be the case and FCNC occur **RP: at tree level**.

The BGL model is based on a symmetry imposed on the whole of the Lagrangian, where some of the quark and scalar fields transform as

$$Q_{L1} \rightarrow e^{i\theta} Q_{L1}, \quad p_{R1} \rightarrow e^{2i\theta} p_{R1}, \quad \Phi_2 \rightarrow e^{i\theta} \Phi_2, \tag{8}$$

with  $\theta \neq n\pi$ , with  $n$  an arbitrary integer. All other fields remain invariant under this symmetry. As we see, the symmetry treats differently one of the generations of quarks <sup>2</sup>, since only the “first family” of quarks is affected by the transformations above. In fact, there are six (not counting the leptonic sector) models of BGL type, which depend which generation of quarks is chosen above. For the scalar sector, the above symmetry transformation yields a Peccei-Quinn [25] scalar potential, which must be complemented with a soft breaking parameter as to yield a massive pseudoscalar particle.

In the fermion sector the impact of the symmetry transformations of eq. (8) is to set to zero several entries of the Yukawa matrices of eq. (1). They are found to be

$$\begin{aligned}
\Gamma_1 &= \begin{pmatrix} 0 & 0 & 0 \\ \times & \times & \times \\ \times & \times & \times \end{pmatrix}, & \Gamma_2 &= \begin{pmatrix} \times & \times & \times \\ 0 & 0 & 0 \\ 0 & 0 & 0 \end{pmatrix}, \\
\Delta_1 &= \begin{pmatrix} 0 & 0 & 0 \\ 0 & \times & \times \\ 0 & \times & \times \end{pmatrix}, & \Delta_2 &= \begin{pmatrix} \times & 0 & 0 \\ 0 & 0 & 0 \\ 0 & 0 & 0 \end{pmatrix},
\end{aligned} \tag{9}$$

where “ $\times$ ” indicates a generic non-zero entry. Then, the form of  $\Delta_1$  and  $\Delta_2$  implies that the matrix  $M_p$  is block diagonal, namely

$$M_p = \begin{pmatrix} \times & 0 & 0 \\ 0 & \times & \times \\ 0 & \times & \times \end{pmatrix}. \tag{10}$$

and it may be bi-diagonalized by matrices  $V_L$  and  $V_R$  of the form

$$V_L = \begin{pmatrix} 1 & 0 & 0 \\ 0 & \times & \times \\ 0 & \times & \times \end{pmatrix}, \quad V_R = \begin{pmatrix} e^{i\theta_R} & 0 & 0 \\ 0 & \times & \times \\ 0 & \times & \times \end{pmatrix}. \tag{11}$$

---

<sup>2</sup>In fact these are unrotated quark fields, not yet corresponding to physical quarks, but the principle holds.

with some phase  $\theta_R$ . The shape of  $V_L$  is crucial for the FCNC suppression. First, though, we see that the matrices  $V_L$  and  $V_R$  can simultaneously bi-diagonalize  $\Delta_1$  and  $\Delta_2$ , and therefore  $M_u$  and  $N_u$  are both diagonal in the basis of physical up quarks. A simple calculation yields

$$N_u = \left( -\frac{m_{u1}}{\tan \beta}, m_{u2} \tan \beta, m_{u3} \tan \beta \right), \quad (12)$$

with  $m_{u1,2,3}$  the masses of the up-type quarks, but we have not yet specified which generation is affected by the BGL transformations. Nevertheless, the above shows that for any choice of transformations in eq. (8) the  $N_u$  matrix is diagonal in the up-type quark mass basis, and therefore – since this matrix contains the quark Yukawa couplings of the neutral scalars – *no FCNC occurs in the up sector*.

The down sector is a different story: given the form of the  $V_L$  matrix in eq. (11) and with the CKM matrix  $V$  given by (5), we immediately obtain

$$U_L = \begin{pmatrix} V(1,1) & V(1,2) & V(1,3) \\ \times & \times & \times \\ \times & \times & \times \end{pmatrix}, \quad (13)$$

and the impact of this structure for the left rotation matrix for the down sector is considerable: a straightforward calculation yields, for the  $N_d$  matrix (which, we remind the reader, contains the Yukawa couplings between physical down-type quarks and scalars)

$$(N_d)_{aa} = m_a \left( \tan \beta - \frac{|V_{1a}|^2}{\sin \beta \cos \beta} \right), \quad (14)$$

for the diagonal terms, where the off-diagonal ones are given by

$$(N_d)_{ab} = -\frac{V_{1a}^* V_{1b}}{\sin \beta \cos \beta} m_k \quad (a \neq b). \quad (15)$$

Thus we see that the off-diagonal Yukawa couplings between scalars and down-type quarks – which are indeed the strength of the FCNC interactions – are CKM-suppressed. There is a freedom to choose the “1” family as any one of the physical quark generations, and therefore one has three BGL models with FCNC in the down sector and without it in the up sector. An analogous symmetry to that of eq. (8) yields another three models, where FCNC now occurs associated with a given family of up-type quarks but where no FCNC occurs for down-type quarks.

This then is how the hallmark of the BGL models is achieved: a flavour-breaking symmetry, which yields off-diagonal FCNC couplings naturally suppressed by the entries of the CKM matrix elements. We will now build a similar model, but with three Higgs doublets.

### 3 A BGL-like 3HDM

Beyond the aesthetic reason of considering three Higgs doublets in analogy with three fermion families, or the intellectual challenge of attempting to reproduce the BGL structure with a larger scalar sector, there are other reasons to attempt a 3HDM with similarly suppressed FCNCs. The BGL model is quite successful, but recent studies [16] have found that its parameter space may be quite constrained. A possible criticism one may levy at the analysis of [16] is that it extended the BGL structure to the leptonic sector as well, something which is not mandatory – the model has enough freedom to have a flavour-preserving leptonic sector in what concerns the scalars, which is what we will consider here. Nonetheless, this shows that even with natural FCNC coupling suppression via off-diagonal CKM matrix elements, the BGL structure can be quite constrained from experimental data. Working within the framework of a 3HDM will in principle imply greater freedom in terms of parameters that can be adjusted to comply with experimental bounds.

There is also another reason, more theoretical and fundamental, to attempt a 3HDM study of the BGL paradigm. In many instances, comparisons of the 2HDM with 3HDMs have revealed how special a model the 2HDM is. To give only a few examples, tree-level vacuum stability against charge breaking or spontaneous CP breaking was found for charge-and-CP conserving minima within the 2HDM [27–29], but charge breaking minima were found to coexist with charge-preserving ones for NHDMS with  $N \geq 3$  [30]; a full listing of all possible symmetries of the  $SU(2) \times U(1)$  invariant 2HDM was found [31, 32] but the same has not yet been possible to accomplish for the 3HDM [20, 33]; generic bounded-from-below [31, 32] and unitarity [34] bounds were found for the 2HDM, but for the 3HDM such bounds only exist for particular versions of the model. As such, the possibility of ascertaining whether the BGL structure can be extended to a full 3HDM compels us to try to find it. And of course one can obtain an *exact* BGL-like 3HDM – all one needs to do is copying the procedure detailed in the previous section for the first two doublets, all the while keeping the last doublet vevless. For that to happen one would take a page from the construction of the Inert Doublet Model (IDM) [35–38] and impose a  $Z_2$  symmetry on the third doublet,  $\phi_3 \rightarrow -\phi_3$ . This model would have FCNCs in the visible sector and also a dark matter candidate stemming from the third doublet. An interesting model to be sure, but it would not solve our aim to obtain a larger freedom to fit the flavour observables than one has in the 2HDM BGL. Thus we are compelled to consider a 3HDM wherein all doublets acquire VEVs.

Let us start by describing the scalar sector of the model, which contains three spin-0  $SU(2)$  doublets,  $\phi_1$ ,  $\phi_2$  and  $\phi_3$ .

### 3.1 The scalar potential

The scalar doublets are made to transform under the  $U(1) \times Z_2$  symmetry as follows:

$$U(1) : \phi_1 \rightarrow e^{i\alpha} \phi_1, \quad \phi_3 \rightarrow e^{i\alpha} \phi_3. \quad (16a)$$

$$Z_2 : \phi_1 \rightarrow -\phi_1, \quad \phi_2 \rightarrow \phi_2, \quad \phi_3 \rightarrow \phi_3. \quad (16b)$$

We further require the scalar potential to be CP-invariant, *i.e* to be invariant under the usual CP transformations,

$$\phi_1 \rightarrow \phi_1^*, \quad \phi_2 \rightarrow \phi_2^*, \quad \phi_3 \rightarrow \phi_3^*. \quad (17)$$

The scalar potential that follows from these symmetry choices can be written as

$$\begin{aligned} V(\phi) = & -\mu_1^2 (\phi_1^\dagger \phi_1) - \mu_2^2 (\phi_2^\dagger \phi_2) - \mu_3^2 (\phi_3^\dagger \phi_3) + \mu_{23}^2 (\phi_2^\dagger \phi_3 + \text{h.c.}) + \lambda_1 (\phi_1^\dagger \phi_1)^2 \\ & + \lambda_2 (\phi_2^\dagger \phi_2)^2 + \lambda_3 (\phi_3^\dagger \phi_3)^2 + \lambda_4 (\phi_1^\dagger \phi_1) (\phi_2^\dagger \phi_2) + \lambda_5 (\phi_1^\dagger \phi_1) (\phi_3^\dagger \phi_3) \\ & + \lambda_6 (\phi_2^\dagger \phi_2) (\phi_3^\dagger \phi_3) + \lambda_7 (\phi_1^\dagger \phi_2) (\phi_2^\dagger \phi_1) + \lambda_8 (\phi_1^\dagger \phi_3) (\phi_3^\dagger \phi_1) + \lambda_9 (\phi_2^\dagger \phi_3) (\phi_3^\dagger \phi_2) \\ & + \lambda_{10} \left\{ (\phi_1^\dagger \phi_3)^2 + \text{h.c.} \right\}, \end{aligned} \quad (18)$$

where due to the CP symmetry all the parameters are real. We have introduced a real soft breaking term, with the  $\mu_{23}^2$  parameter, to avoid the appearance of a massless axion. Recall that the same procedure was necessary for the 2HDM BGL, due to the analogous breaking of the  $U(1)$  symmetry given by eq. (8). After spontaneous symmetry breaking (SSB), all doublets acquire real VEVs <sup>3</sup> and are expanded as

$$\phi_k = \left( \frac{w_k^+}{\sqrt{2}} (v_k + h_k + iz_k) \right), \quad (k = 1, 2, 3) \quad (19)$$

where  $v_k$  represents VEVs of each doublet, which obviously satisfy  $v_1^2 + v_2^2 + v_3^2 = (246 \text{ GeV})^2$ . The minimization of the potential yields three equations which means that one can express the quadratic parameters  $\mu_1^2$ ,  $\mu_2^2$  and

---

<sup>3</sup>It is obviously possible to obtain spontaneous CP violation within 3HDMs, which originates complex vevs, but we will not be considering that case in this work.

$\mu_3^2$  in favor of the three VEVs and other couplings as follows:

$$\mu_1^2 = \lambda_1 v_1^2 + \frac{1}{2} (\lambda_4 + \lambda_7) v_2^2 + \frac{1}{2} (\lambda_5 + \lambda_8 + 2\lambda_{10}) v_2^2, \quad (20a)$$

$$\mu_2^2 = \lambda_2 v_2^2 + \frac{1}{2} (\lambda_4 + \lambda_7) v_1^2 + \frac{1}{2} (\lambda_6 + \lambda_9) v_3^2 + \frac{v_3}{v_2} \mu_{23}^2, \quad (20b)$$

$$\mu_3^2 = \lambda_3 v_3^2 + \frac{1}{2} (\lambda_6 + \lambda_9) v_2^2 + \frac{1}{2} (\lambda_5 + \lambda_8 + 2\lambda_{10}) v_1^2 + \frac{v_2}{v_3} \mu_{23}^2. \quad (20c)$$

For latter use, we also parameterize the VEVs as

$$v_1 = v \cos \psi_1 \cos \psi_2, \quad v_2 = v \sin \psi_1 \cos \psi_2, \quad v_3 = v \sin \psi_2, \quad (21)$$

where  $v = \sqrt{v_1^2 + v_2^2 + v_3^2}$ . We also define the following orthogonal matrix which will simplify our analysis of the pseudoscalar and the charged scalar sectors:

$$O = \begin{pmatrix} \cos \psi_2 \cos \psi_1 & \cos \psi_2 \sin \psi_1 & \sin \psi_2 \\ -\sin \psi_1 & \cos \psi_1 & 0 \\ -\cos \psi_1 \sin \psi_2 & -\sin \psi_1 \sin \psi_2 & \cos \psi_2 \end{pmatrix}. \quad (22)$$

We now turn our attention to the physical scalar spectrum of the model. Since we are considering a potential with explicit CP conservation and a vacuum which does not spontaneously break CP (all vevs were taken real), the neutral scalars have definite Cp quantum numbers, and the scalar spectrum of the model is composed of: a pair of pseudoscalars; a trio of CP-even scalars; and a pair of charged scalars.

### 3.1.1 CP-odd scalar sector

The mass terms for the pseudoscalar sector can be extracted from the scalar potential easily – they will correspond to the terms quadratic in the  $z$  fields, after one has replaced the expression for the doublets of eq. (19) into the potential (18). One obtains

$$V_P^{\text{mass}} = (z_1 \ z_2 \ z_3) \frac{M_P^2}{2} \begin{pmatrix} z_1 \\ z_2 \\ z_3 \end{pmatrix}, \quad (23)$$

where  $M_P^2$  is the  $3 \times 3$  pseudoscalar mass matrix, which can be block diagonalized as:

$$B_P^2 \equiv O \cdot M_P^2 \cdot O^T = \begin{pmatrix} 0 & 0 & 0 \\ 0 & (B_P^2)_{22} & (B_P^2)_{23} \\ 0 & (B_P^2)_{23} & (B_P^2)_{33} \end{pmatrix}. \quad (24a)$$

The line and column of zeroes in this matrix obviously tells us that it has a zero eigenvalue – which of course is the neutral Goldstone boson responsible for the mass of the  $Z$  boson. The elements of  $B_P^2$  are given by, after minor calculations,

$$(B_P^2)_{22} = \frac{v_3(-2v_2^3 v_3 \lambda_{10} + v_1^2 \mu_{23}^2)}{v_2(v_1^2 + v_2^2)}, \quad (24b)$$

$$(B_P^2)_{23} = -\frac{v_1 v(2v_2 v_3 \lambda_{10} + \mu_{23}^2)}{v_1^2 + v_2^2}, \quad (24c)$$

$$(B_P^2)_{33} = -\frac{v^2(2v_1^2 v_3 \lambda_{10} - v_2 \mu_{23}^2)}{(v_1^2 + v_2^2)v_3}. \quad (24d)$$

From the above equations we notice that, apart from the three VEVs, only  $\lambda_{10}$  and  $\mu_{23}^2$  enter in the pseudoscalar mass matrix. We can solve for these two parameters from the trace and the determinant of the  $2 \times 2$  block to obtain:

$$\text{Tr}(B_P^2) = m_{A1}^2 + m_{A2}^2 = -2\lambda_{10}v^2(1 - s_{\psi_1}^2 c_{\psi_2}^2) + \frac{\mu_{23}^2}{s_{\psi_1} s_{\psi_2} c_{\psi_2}} (1 - c_{\psi_1}^2 c_{\psi_2}^2), \quad (25a)$$

$$\text{Det}(B_P^2) = m_{A1}^2 m_{A2}^2 = -2\lambda_{10} v^2 \frac{\mu_{23}^2 s_{\psi_2}}{s_{\psi_1} c_{\psi_2}}, \quad (25b)$$

where  $m_{A1}^2$  and  $m_{A2}^2$  are the physical pseudoscalar masses. Eqs. (25) therefore allow us to express two of the parameters of the potential (18) in terms of two physical masses and mixing angles  $\psi$ .

PF: Please check whether the following is correct, I added it here thinking it would be useful. Not sure if this is in agreement with Ludwig's notation, do we wish to uniformize already? The gamma angles would be swapped, I think, and the matrix  $O$  would become  $O_\beta$ ? The full diagonalization of the pseudoscalar mass matrix is then obtained via an additional rotation,

$$O_{\gamma_1} \cdot B_P^2 \cdot O_{\gamma_1}^T = \begin{pmatrix} 0 & 0 & 0 \\ 0 & m_{A1}^2 & 0 \\ 0 & 0 & m_{A2}^2 \end{pmatrix}, \quad (26)$$

where the rotation matrix  $O_{\gamma_1}$  is defined as

$$O_{\gamma_1} = \begin{pmatrix} 1 & 0 & 0 \\ 0 & \cos \gamma_1 & -\sin \gamma_1 \\ 0 & \sin \gamma_1 & \cos \gamma_1 \end{pmatrix}. \quad (27)$$

The full diagonalization of  $M_P^2$  from eq. (23) is therefore accomplished with the matrix product  $O \cdot O_{\gamma_1}$ , and this is important when one wishes to write the Yukawa interactions between the two physical pseudoscalars and the physical quarks.

### 3.1.2 Charged scalar sector

Similarly to the pseudoscalar case, the  $3 \times 3$  charged sector mass matrix,  $M_C^2$ , can also be block diagonalized as:

$$B_C^2 \equiv O \cdot M_C^2 \cdot O^T = \begin{pmatrix} 0 & 0 & 0 \\ 0 & (B_C^2)_{22} & (B_C^2)_{23} \\ 0 & (B_C^2)_{23} & (B_C^2)_{33} \end{pmatrix}. \quad (28a)$$

where again the single line and column of zeros yields a zero eigenvalue, the massless charged Goldstone boson responsible for the mass of the  $W$ . The remaining elements of the matrix are found to be

$$(B_C^2)_{22} = -\frac{1}{2v_2(v_1^2 + v_2^2)} [v_2^5 \lambda_7 + v_2^3 (2v_1^2 \lambda_7 + v_3^2 (2\lambda_{10} + \lambda_8)) + v_2 (v_1^4 \lambda_7 + v_1^2 v_3^2 \lambda_9) - 2v_1^2 v_3 \mu_{23}^2], \quad (28b)$$

$$(B_C^2)_{23} = -\frac{v_1 v}{2(v_1^2 + v_2^2)} [v_2 v_3 (2\lambda_{10} + \lambda_8 - \lambda_9) + 2\mu_{23}^2], \quad (28c)$$

$$(B_C^2)_{33} = -\frac{v^2}{2(v_1^2 + v_2^2)v_3} [v_1^2 v_3 (2\lambda_{10} + \lambda_8) + v_2 (v_2 v_3 \lambda_9 - 2\mu_{23}^2)]. \quad (28d)$$

We completely diagonalize the charged scalar mass matrix as,

$$O_{\gamma_2} \cdot (B_C)^2 \cdot O_{\gamma_2}^T = \begin{pmatrix} 0 & 0 & 0 \\ 0 & m_{C1}^2 & 0 \\ 0 & 0 & m_{C2}^2 \end{pmatrix}, \quad (29a)$$

where

$$O_{\gamma_2} = \begin{pmatrix} 1 & 0 & 0 \\ 0 & \cos \gamma_2 & -\sin \gamma_2 \\ 0 & \sin \gamma_2 & \cos \gamma_2 \end{pmatrix}, \quad (29b)$$

and  $m_{C1}$  and  $m_{C2}$  denote the masses of the two physical charged scalars,  $H_1^\pm$  and  $H_2^\pm$ , respectively. Thus, we will have the following relations:

$$m_{C1}^2 \cos^2 \gamma_2 + m_{C2}^2 \sin^2 \gamma_2 = (B_C^2)_{22}, \quad (30a)$$

$$\cos \gamma_2 \sin \gamma_2 (m_{C2}^2 - m_{C1}^2) = (B_C^2)_{23}, \quad (30b)$$

$$m_{C1}^2 \sin^2 \gamma_2 + m_{C2}^2 \cos^2 \gamma_2 = (B_C^2)_{33}. \quad (30c)$$

These equations, in conjunction with eq. (28) will enable us to solve for  $\lambda_7$ ,  $\lambda_8$ , and  $\lambda_9$  as given below:

$$\lambda_7 = \frac{s_{2\psi_1}}{v^2 s_{\psi_1} c_{\psi_1} c_{\psi_2}^2} [(s_{\psi_2}^2 s_{\gamma_2}^2 - c_{\gamma_2}^2) m_{C1}^2 + (s_{\psi_2}^2 c_{\gamma_2}^2 - s_{\gamma_2}^2) m_{C2}^2 + s_{\psi_2} \cot 2\psi_1 s_{2\gamma_2} (m_{C1}^2 - m_{C2}^2)], \quad (31a)$$

$$\lambda_8 = \frac{2}{v^2} \left[ \frac{s_{\psi_1} c_{\gamma_2} s_{\gamma_2}}{s_{\psi_2} c_{\psi_1}} (m_{C1}^2 - m_{C2}^2) - (s_{\gamma_2}^2 m_{C1}^2 + c_{\gamma_2}^2 m_{C2}^2) \right] - 2\lambda_{10}, \quad (31b)$$

$$\lambda_9 = \frac{2}{v^2} \left[ \frac{\mu_{23}^2}{s_{\psi_1} s_{\psi_2} c_{\psi_2}} - \frac{c_{\psi_1} c_{\gamma_2} s_{\gamma_2}}{s_{\psi_2} s_{\psi_1}} (m_{C1}^2 - m_{C2}^2) - (s_{\gamma_2}^2 m_{C1}^2 + c_{\gamma_2}^2 m_{C2}^2) \right]. \quad (31c)$$

where the  $\lambda_{10}$  and  $\mu_{23}^2$  can be replaced using eq. (25). Therefore, another three parameters of the potential are expressed in terms of physical masses and mixing angles.

### 3.1.3 CP-even scalar sector

Repeating the procedure of the previous sections for the CP-even states, we obtain

$$V_S^{\text{mass}} = (h_1 \ h_2 \ h_3) \frac{M_S^2}{2} \begin{pmatrix} h_1 \\ h_2 \\ h_3 \end{pmatrix}, \quad (32a)$$

where  $M_S^2$  is a  $3 \times 3$  symmetric mass matrix whose elements are given by:

$$(M_S^2)_{11} = 2v_1^2 \lambda_1, \quad (32b)$$

$$(M_S^2)_{12} = v_1 v_2 (\lambda_4 + \lambda_7), \quad (32c)$$

$$(M_S^2)_{13} = v_1 v_3 (2\lambda_{10} + \lambda_5 + \lambda_8), \quad (32d)$$

$$(M_S^2)_{22} = 2v_2^2 \lambda_2 + \frac{v_3 \mu_{23}^2}{v_2}, \quad (32e)$$

$$(M_S^2)_{23} = v_2 v_3 (\lambda_6 + \lambda_9) - \mu_{23}^2, \quad (32f)$$

$$(M_S^2)_{33} = 2v_3^2 \lambda_3 + \frac{v_2 \mu_{23}^2}{v_3}. \quad (32g)$$

The physical  $CP$  even scalars,  $h$ ,  $H_1$  and  $H_2$ , are obtained via the following orthogonal rotation:

$$\begin{pmatrix} h \\ H_1 \\ H_2 \end{pmatrix} = O_\alpha \begin{pmatrix} h_1 \\ h_2 \\ h_3 \end{pmatrix}, \quad (33)$$

where  $O_\alpha$  is a  $3 \times 3$  orthogonal matrix which can be conveniently parameterized as

$$O_\alpha = R_3 \cdot R_2 \cdot R_1, \quad (34a)$$

with,

$$R_1 = \begin{pmatrix} \cos \alpha_1 & \sin \alpha_1 & 0 \\ -\sin \alpha_1 & \cos \alpha_1 & 0 \\ 0 & 0 & 1 \end{pmatrix}, \quad R_2 = \begin{pmatrix} \cos \alpha_2 & 0 & \sin \alpha_2 \\ 0 & 1 & 0 \\ -\sin \alpha_2 & 0 & \cos \alpha_2 \end{pmatrix}, \quad R_3 = \begin{pmatrix} 1 & 0 & 0 \\ 0 & \cos \alpha_3 & \sin \alpha_3 \\ 0 & -\sin \alpha_3 & \cos \alpha_3 \end{pmatrix}. \quad (34b)$$

Therefore  $M_S^2$  should be diagonalized via the following orthogonal transformation:

$$O_\alpha \cdot M_S^2 \cdot O_\alpha^T \equiv \begin{pmatrix} m_h^2 & 0 & 0 \\ 0 & m_{H1}^2 & 0 \\ 0 & 0 & m_{H2}^2 \end{pmatrix}. \quad (35)$$

Inverting the above equation we get,

$$M_S^2 \equiv O_\alpha^T \cdot \begin{pmatrix} m_h^2 & 0 & 0 \\ 0 & m_{H1}^2 & 0 \\ 0 & 0 & m_{H2}^2 \end{pmatrix} \cdot O_\alpha, \quad (36)$$

which enables us to solve for the remaining six  $\lambda$  couplings, obtaining

$$\lambda_1 = \frac{1}{2v^2} \left[ \left( \frac{c_{\alpha_1} c_{\alpha_2}}{c_{\psi_1} c_{\psi_2}} \right)^2 m_h^2 + \left( \frac{c_{\alpha_3} s_{\alpha_1} + c_{\alpha_1} s_{\alpha_2} s_{\alpha_3}}{s_{\psi_1} c_{\psi_2}} \right)^2 m_{H1}^2 + \left( \frac{c_{\alpha_1} c_{\alpha_3} s_{\alpha_2} - s_{\alpha_1} s_{\alpha_3}}{c_{\psi_1} c_{\psi_2}} \right)^2 m_{H2}^2 \right], \quad (37a)$$

$$\begin{aligned} \lambda_2 = & \frac{1}{2v^2} \left[ -\frac{\mu_{23}^2 s_{\psi_2}}{s_{\psi_1}^3 c_{\psi_2}^3} + \left( \frac{c_{\alpha_2} s_{\alpha_1}}{s_{\psi_1} c_{\psi_2}} \right)^2 m_h^2 + \left( \frac{c_{\alpha_1} c_{\alpha_3} - s_{\alpha_1} s_{\alpha_2} s_{\alpha_3}}{s_{\psi_1} c_{\psi_2}} \right)^2 m_{H1}^2 \right. \\ & \left. + \left( \frac{c_{\alpha_3} s_{\alpha_1} s_{\alpha_2} + c_{\alpha_1} s_{\alpha_3}}{s_{\psi_1} c_{\psi_2}} \right)^2 m_{H2}^2 \right], \end{aligned} \quad (37b)$$

$$\lambda_3 = \frac{1}{2v^2} \left[ \frac{\mu_{23}^2 c_{\psi_2} s_{\psi_1}}{s_{\psi_2}^2} + \frac{s_{\gamma_2}^2}{s_{\psi_2}^2} m_h^2 + \frac{c_{\gamma_2}^2}{s_{\psi_2}^2} (s_{\gamma_3}^2 m_{H1}^2 + c_{\gamma_3}^2 m_{H2}^2) \right], \quad (37c)$$

$$\begin{aligned} \lambda_4 = & \frac{c_{\gamma_1} c_{\gamma_2}^2 s_{\gamma_1}}{v^2 s_{\psi_1} c_{\psi_2}^2 c_{\psi_1}} m_h^2 - \frac{1}{v^2 s_{\psi_1} c_{\psi_2}^2 c_{\psi_1}} \left[ (c_{\alpha_3} s_{\alpha_1} + c_{\alpha_1} s_{\alpha_2} s_{\alpha_3})(c_{\alpha_1} c_{\alpha_3} - s_{\alpha_1} s_{\alpha_2} s_{\alpha_3}) m_{H1}^2 \right. \\ & \left. - (c_{\alpha_3} s_{\alpha_1} s_{\alpha_2} + c_{\alpha_1} s_{\alpha_3})(c_{\alpha_1} c_{\alpha_3} s_{\alpha_2} - s_{\alpha_1} s_{\alpha_3}) m_{H2}^2 \right] - \lambda_7, \end{aligned} \quad (37d)$$

$$\begin{aligned} \lambda_5 = & \frac{c_{\alpha_2} c_{\alpha_1} s_{\alpha_2}}{v^2 s_{\psi_2} c_{\psi_1} c_{\psi_2}} m_h^2 - \frac{1}{v^2} \left[ s_{\alpha_3} (c_{\alpha_3} s_{\alpha_1} + c_{\alpha_1} s_{\alpha_2} s_{\alpha_3}) m_{H1}^2 - c_{\alpha_3} (s_{\alpha_1} s_{\alpha_3} - c_{\alpha_1} c_{\alpha_3} s_{\alpha_2}) m_{H2}^2 \right] \\ & - 2\lambda_{10} - \lambda_8, \end{aligned} \quad (37e)$$

$$\begin{aligned} \lambda_6 = & \frac{c_{\alpha_2} s_{\alpha_1} s_{\alpha_2}}{v^2 s_{\psi_1} s_{\psi_2} c_{\psi_2}} m_h^2 + \frac{1}{v^2 s_{\psi_1} s_{\psi_2} c_{\psi_2}} \left[ \mu_{23}^2 + c_{\alpha_2} s_{\alpha_3} (c_{\alpha_1} c_{\alpha_3} - s_{\alpha_1} s_{\alpha_2} s_{\alpha_3}) m_{H1}^2 \right. \\ & \left. - c_{\alpha_2} c_{\alpha_3} (c_{\alpha_3} s_{\alpha_1} s_{\alpha_2} - c_{\alpha_1} s_{\alpha_3}) m_{H2}^2 \right] - \lambda_9, \end{aligned} \quad (37f)$$

where the potential parameters appearing on the r.h.s. can be replaced using Eqs. (25) and (31).

At this point, it is instructive to count the number of parameters in the scalar sector. We note that the scalar potential of Eq. (18) contains fourteen real parameters. Among them, the quadratic parameters  $\mu_1^2$ ,  $\mu_2^2$  and  $\mu_3^2$  can be traded in favor of the three VEVs,  $v_1$ ,  $v_2$  and  $v_3$  or equivalently  $v$ ,  $\tan \psi_1$  and  $\tan \psi_2$ . Two more parameters,  $\mu_{23}^2$  and  $\lambda_{10}$ , can be exchanged for  $m_{A1}$  and  $m_{A2}$  using Eq. (25). The remaining nine quartic couplings, as shown in Eqs. (31) and (37), can be expressed in terms of five physical masses (three CP-even scalars, and two charged scalars) and three mixing angles (three in the CP-even sector and one in the charged scalar sector). In these relations, putting  $m_h = 125$  GeV,  $\alpha_1 = \psi_1$  and  $\alpha_2 = \psi_2$  will ensure the presence of a 125 GeV SM like scalar in the spectrum [39] - that is the *exact* alignment limit of this model, forcing the interactions between  $h$  and the electroweak gauge bosons  $Z$  and  $W$  to be exactly identical to those of the SM.

**PF: also those of the fermions?**

### 3.2 The Yukawa sector

Alongside the scalar field transformations of eq. (16) the following quark fields are assumed to transform nontrivially under the  $U(1) \times Z_2$  flavor symmetry:

$$U(1) : Q_{L3} \rightarrow e^{i\alpha} Q_{L3}, \quad p_{R3} \rightarrow e^{2i\alpha} p_{R3}, \quad (38a)$$

$$Z_2 : Q_{L3} \rightarrow -Q_{L3}, \quad p_{R3} \rightarrow -p_{R3}, \quad n_{R3} \rightarrow -n_{R3}, \quad (38b)$$

with  $\alpha$  the same arbitrary phase of eq. (16), and the rest of the quark fields remain unaffected under said symmetry transformations. In Eq. (38), as before,  $Q_{La} = (p_{La}, n_{La})^T$  denotes the left-handed quark doublet of  $a$ -th generation whereas  $p_{Ra}$  and  $n_{Ra}$  denote the  $a$ -th generation (unrotated) up and down type quark singlets respectively. Notice the similarity between these transformation laws and those of the BGL model, eq. (8).

The quark Yukawa Lagrangian for a 3HDM will then have the general form

$$\mathcal{L}_Y = - \sum_{k=1}^3 \left[ \bar{Q}_{La}(\Gamma_k)_{ab} \phi_k n_{Rb} + \bar{Q}_{La}(\Gamma_k)_{ab} \tilde{\phi}_k p_{Rb} + \text{h.c.} \right], \quad (39)$$

where as before  $\Gamma_k$  and  $\Delta_k$  stand for the Yukawa matrices in the down and up quark sectors respectively. Because of the assigned charges under  $U(1) \times Z_2$  these Yukawa matrices will have the following textures:

$$\Gamma_1 = \begin{pmatrix} 0 & 0 & 0 \\ 0 & 0 & 0 \\ \times & \times & 0 \end{pmatrix}, \quad \Delta_1 = \begin{pmatrix} 0 & 0 & 0 \\ 0 & 0 & 0 \\ 0 & 0 & 0 \end{pmatrix}, \quad \Gamma_2, \Delta_2 = \begin{pmatrix} \times & \times & 0 \\ \times & \times & 0 \\ 0 & 0 & 0 \end{pmatrix}, \quad \Gamma_3, \Delta_3 = \begin{pmatrix} 0 & 0 & 0 \\ 0 & 0 & 0 \\ 0 & 0 & \times \end{pmatrix}. \quad (40)$$

Therefore, the quark mass matrices that emerge from these Yukawa matrices have the following structure:

$$M_p = \frac{1}{\sqrt{2}} \sum_{k=1}^3 \Delta_k v_k = \begin{pmatrix} \times & \times & 0 \\ \times & \times & 0 \\ 0 & 0 & \times \end{pmatrix}, \quad M_n = \frac{1}{\sqrt{2}} \sum_{k=1}^3 \Gamma_k v_k = \begin{pmatrix} \times & \times & 0 \\ \times & \times & 0 \\ \times & \times & \times \end{pmatrix}. \quad (41)$$

We then rotate from the  $p$  and  $n$  fields to the physical quark states  $u$  and  $d$  via rotation matrices  $V_L$ ,  $V_R$ ,  $U_L$  and  $U_R$  identical to those of eq. (4). We thus obtain diagonal mass matrices as in eq. (3), and the CKM matrix is, as before, given by  $V = V_L^\dagger U_L$ . Let us now analyse carefully the Yukawa couplings between the neutral scalar eigenstates and the physical quarks, with particular attention to any FCNC couplings which may arise.

For a first approximation to the FCNC couplings, let us define the following intermediate basis for the  $CP$ -even scalars:

$$\begin{pmatrix} H_0 \\ H'_1 \\ H'_2 \end{pmatrix} = \begin{pmatrix} v_1/v & v_2/v & v_3/v \\ v_3/v_{13} & 0 & -v_1/v_{13} \\ v_1 v_2 / (v v_{13}) & -v_{13}/v & v_2 v_3 / (v v_{13}) \end{pmatrix} \begin{pmatrix} h_1 \\ h_2 \\ h_3 \end{pmatrix}, \quad (42)$$

where  $v_{13} = \sqrt{v_1^2 + v_3^2}$ . As we will show, the state  $H_0$  will have SM like Yukawa couplings at tree level. In the alignment limit, with  $\alpha_1 = \psi_1$  and  $\alpha_2 = \psi_2$ , the physical scalar  $h$  completely overlaps with  $H_0$ . In that limit, the other physical scalars,  $H_1$  and  $H_2$ , will, in general, be an orthogonal mixture of the intermediate states defined above,  $H'_1$  and  $H'_2$ .

Now, the terms in the Yukawa lagrangean pertaining to the interactions between  $CP$ -even scalars and quarks are

$$\mathcal{L}_Y^{CP \text{ even}} = -\frac{1}{\sqrt{2}} \left[ \bar{n}_L \left( \sum_{k=1}^3 \Gamma_k h_k \right) n_R + \bar{p}_L \left( \sum_{k=1}^3 \Delta_k h_k \right) p_R + \text{h.c.} \right], \quad (43)$$

from which, using the rotation matrix of eq. (42) to express the  $h_k$  in terms of  $H_0$ , we can obtain

$$\mathcal{L}_Y^{H_0} = -\frac{H_0}{v} \left[ \bar{n}_L \left( \frac{1}{\sqrt{2}} \sum_{k=1}^3 \Gamma_k v_k \right) n_R + \bar{p}_L \left( \frac{1}{\sqrt{2}} \sum_{k=1}^3 \Delta_k v_k \right) p_R + \text{h.c.} \right], \quad (44)$$

$$= -\frac{H_0}{v} [\bar{d}_L D_d d_R + \bar{u}_L D_u u_R + \text{h.c.}] . \quad (45)$$

In writing the last step, we have made use of Eqs. (41) and (3). Thus we see that  $H_0$  possesses SM like Yukawa coupling at tree level. This is a close analogy to the BGL model, where we explained how, in the exact 2HDM alignment limit, the  $h$  state had identical Yukawa interactions to those of the SM Higgs boson.

In a similar manner, we can write down the Yukawa couplings of  $H'_1$  and  $H'_2$  with the down type quarks as follows:

$$\mathcal{L}_Y^{H'_1, H'_2} = -\frac{H'_1}{v} \bar{d}_L N_{d1} d_R - \frac{H'_2}{v} \bar{d}_L N_{d2} d_R + \text{h.c.}, \quad (46)$$

where the matrices  $N_{d1}$  and  $N_{d2}$  are given by

$$N_{d1} = \frac{v}{\sqrt{2}v_{13}} U_L^\dagger (\Gamma_1 v_3 - \Gamma_3 v_1) U_R, \quad (47a)$$

$$N_{d2} = U_L^\dagger \left[ \frac{v_2}{v_{13}} \frac{1}{\sqrt{2}} (\Gamma_1 v_1 + \Gamma_3 v_3) - \frac{v_{13}}{v_2} \frac{1}{\sqrt{2}} \Gamma_2 v_2 \right] U_R. \quad (47b)$$

To simplify further the expressions for  $N_{d1}$  and  $N_{d2}$ , we go back to the textures of the mass matrices in Eq. (41). From the block diagonal structure of  $M_u$ , one can conclude that the corresponding bidiagonalizing matrices,  $V_L$  and  $V_R$ , should have block diagonal structures too. In fact, we can choose

$$V_L = \begin{pmatrix} \times & \times & 0 \\ \times & \times & 0 \\ 0 & 0 & 1 \end{pmatrix} \quad (48)$$

with the understanding that the phase of  $(M_u)_{33}$  can always be dumped into  $(V_R)_{33}$ . Here, unlike the BGL example of section 2, we are choosing to single out the third family. Then, from Eq. (5) we obtain

$$(U_L)_{3A} = V_{3A}, \quad (49)$$

which means that the third row of  $U_L$  is identical to that of the CKM matrix, as occurred in the 2HDM BGL case. To proceed further, it is useful to define the following projection matrix

$$P = \begin{pmatrix} 0 & 0 & 0 \\ 0 & 0 & 0 \\ 0 & 0 & 1 \end{pmatrix}. \quad (50)$$

Thus, in view of the structures of the Yukawa matrices, we obtain the following relations in the down quark sector:

$$\Gamma_3 = (\Gamma_3)_{33} P, \quad \frac{1}{\sqrt{2}} (\Gamma_1 v_1 + \Gamma_3 v_3) = P M_d. \quad (51)$$

Using Eqs. (49) and (51), the expressions for  $N_{d1}$  and  $N_{d2}$  can now be simplified so that:

$$(N_{d1})_{AB} = \frac{v v_3}{v_1 v_{13}} V_{3A}^* V_{3B} (D_d)_{BB} - \frac{1}{\sqrt{2}} \frac{v v_{13}}{v_1} (\Gamma_3)_{33} V_{3A}^* (U_R)_{3B}, \quad (52a)$$

$$(N_{d2})_{AB} = \frac{v_{13}}{v_2} (D_d)_{BB} \delta_{AB} + \left( \frac{v_{13}}{v_2} + \frac{v_2}{v_{13}} \right) V_{3A}^* V_{3B} (D_d)_{BB}. \quad (52b)$$

These equations tell us that the FCNC interactions of  $H'_2$  are *exactly* BGL-like – all off-diagonal elements in  $N_{d2}$  are CKM-suppressed. That however is not the case for  $H'_1$  – the first term in the right-hand side of eq. (52a) is a matrix whose off-diagonal entries are suppressed by *two* CKM matrix elements, as in the BGL model, but the second term's FCNC couplings are suppressed by only *one* CKM matrix element. To estimate the size of  $(U_R)_{3B}$ , we note that if  $(\Gamma_1)_{31}$  and  $(\Gamma_1)_{32}$  were zero in Eq. (40), then we could choose  $U_R$  to be block diagonal

as well. However, in view of the smallness of the off Cabibbo elements in the CKM matrix, the elements of  $\Gamma_1$  should also be quite small. Therefore it is reasonable to assume that the elements  $(U_R)_{3B}$  (for  $B \neq 3$ ) are also small. Considering all these facts, one can expect that the FCNC couplings in the down quark sector controlled by  $N_{d1}$  and  $N_{d2}$  will be under control. **PF: I added the following, which I think is important** Ultimately, of course, we will be close to the alignment limit – the current LHC data requires it, see section 4.2 – but not *exactly* in it, so the physical CP-even scalar states (and the CP-odd ones too, one might add) will have FCNC interactions given by linear combinations of the  $N_{d1}$  and  $N_{d2}$  matrices via the rotation matrices defined in section 3.1. As such, one obtains a model that isn't as “clean” as the 2HDM BGL, but where one still sees how FCNC interactions arise which are CKM-suppressed due to the symmetries imposed upon the potential – the suppression is therefore natural, not the result of a fine tuning.

A similar exercise in the up quark sector would reveal that there are no scalar mediated FCNC at tree level in the up sector. This is due to the special structures of the up type Yukawa matrices, which, in turn, are dictated by the fermionic charges given in Eq. (38). But it should be noted that, just like in the usual BGL models, the charges in Eq. (38) can be appropriately shuffled so that the tree level FCNC couplings reside entirely in the up quark sector instead of the down quark sector. And within each sector one still has the possibility of choosing FCNC associated with a given family. However, we choose the current variant – FCNC in the down sector, associated with the third family – because it will be the most restrictive one. There is a wealth of experimental data limiting such FCNCs, thus this version of the model will be the most restricted one. Therefore, if this version can survive all constraints we will throw at it, other versions are sure to fare easier and may be the subject of future studies.

In passing, it should be mentioned that the leptonic fields are assumed to couple only to  $\phi_1$  in the Yukawa sector. This can be achieved very simply by assigning the following transformations to the leptonic fields

$$U(1) : L_{La} \rightarrow e^{i\alpha} L_{La}, \quad \ell_{Ra} \rightarrow \ell_{Ra}, \quad (53a)$$

$$Z_2 : L_{La} \rightarrow -L_{La}, \quad \ell_{Ra} \rightarrow \ell_{Ra}, \quad (53b)$$

where  $L_{La} = (\nu_{La}, \ell_{La})^T$  and  $\ell_{Ra}$  denote respectively the left-handed lepton doublet and the right handed charged lepton singlet of  $a$ -th generation. Since the charged leptons receive their masses from a single scalar doublet, there will be no FCNC couplings at tree level in the leptonic sector. Thus all constraints from observables such as  $\mu \rightarrow e\gamma$  are automatically satisfied, since in our model lepton number is conserved. Additionally, it is also worth mentioning that we do not introduce right handed neutrinos, *i.e.*, neutrinos are assumed to be massless in our model.

### 3.3 The Inverted Procedure

One major challenge in producing a BSM theory with a non-trivial Yukawa sector, *i.e.* with FCNC interactions, resides in being able to successfully fit the quark mass spectrum. In fact, it is highly non-trivial – and time-consuming – to find values for Yukawa couplings and scalar vevs capable of fitting quarks masses which differ by many orders of magnitude. Add to that the difficulty in having to simultaneously being capable of fitting the CKM matrix entries and a simultaneous fit to the quark and scalar sector becomes a very difficult achievement. In this work we follow a *inverted procedure* (**PF: IS THERE A DIPANKAR REF. FOR THE INVERTED PROCEDURE?** ) which consists in, literally, inverting the usual fitting logic of the Yukawa sector: instead of scanning over Yukawa couplings and vevs defining some sort of  $\chi^2$  function whose minimisation would yield an acceptable quark mass spectrum and CKM matrix, we do the opposite. Namely, quark masses and CKM matrix elements are our initial inputs, and we scan over the *bidiagonalization matrices* which pass from the interaction basis to the mass eigenstate basis.

To make this clear, let us begin with the diagonal quark mass matrices,  $D_u = \text{diag}(m_u, m_c, m_t)$  and  $D_d = \text{diag}(m_d, m_s, m_b)$ . Within the BGL-like 3HDM, they are the result of the bidiagonalization of the (interaction basis) matrices of eq. (41), via  $3 \times 3$  unitary matrices  $U_L, U_R, V_L$  and  $V_R$  such that

$$D_u = V_L^\dagger M_p V_R \quad , \quad D_d = U_L^\dagger M_n U_R \quad (54)$$

and the CKM matrix is given by the product  $V = V_L^\dagger U_L$ . Using the unitarity of the rotation matrices we can invert the above equations, and since the definition of the CKM matrix implies that  $U_L = V_L V$ , we can write

$$\begin{aligned} M_p &= V_L D_u V_R^\dagger = \begin{pmatrix} (\Delta_2)_{11}v_2 & (\Delta_2)_{12}v_2 & 0 \\ (\Delta_2)_{21}v_2 & (\Delta_2)_{22}v_2 & 0 \\ 0 & 0 & (\Delta_2)_{33}v_3 \end{pmatrix}, \\ M_n &= V_L V D_d U_R^\dagger \begin{pmatrix} (\Gamma_2)_{11}v_2 & (\Gamma_2)_{12}v_2 & 0 \\ (\Gamma_2)_{21}v_2 & (\Gamma_2)_{22}v_2 & 0 \\ (\Gamma_1)_{31}v_1 & (\Gamma_1)_{32}v_1 & (\Gamma_3)_{33}v_3 \end{pmatrix}. \end{aligned} \quad (55)$$

In eq. (55) the quark masses, CKM matrix and vevs will be the inputs (the vevs obtained from a previous partial scan of the scalar sector, already ensuring that the alignment limit is satisfied). The unknowns are the rotation matrices  $V_L$ ,  $V_R$  and  $U_R - U_L$  having been replaced by  $V_L$  and the CKM matrix. Since any  $U(3)$  matrix can be parameterised by three angles and six phases we have a total of 27 free parameters with which to attempt a fit to eq. (55) – in this fit, each zero entry on the matrices explicitly shown has to be reproduced with a given tolerance (namely, those entries will have to be smaller, by many (PF:HOW MANY? IS THIS HOW WE DO IT, WITH FULLY GENERAL U(3) MATRICES, OR IS THERE SOME SIMPLIFICATION CHOOSING PHASES TO BE ZERO?) orders of magnitude, than the smallest non-zero entries). And with the vevs and the values obtained for the non-zero entries, it is a simple matter to reconstruct the nonzero elements of the  $\Gamma$  and  $\Delta$  – notice that each non zero entry of  $M_p$  ( $M_n$ ) has the contribution of a single  $\Delta$  ( $\Gamma$ ) matrix element, so the reconstruction of the Yukawa matrices is unequivocal.

With this simple procedure we ensure that the very different scales of the quark masses are automatically reproduced, as well as the non-trivial structure of the CKM matrix. The computational challenge then becomes to be able to efficiently scan over the nine rotation angles and eighteen complex phases in order to reproduce the textures of the mass matrices.

(PF: IT WOULD BE NICE TO HAVE A "SUCCESS RATE" HERE, SOME IDEA OF HOW OFTEN THE YUKAWA FIT FAILS/SUCCEEDS

## 4 Constraints on the model

Any BSM theory is constrained from having to do at least as good a job as the SM in describing particle interactions. For multiscalar models, there is a wealth of bounds that are imposed upon the model's parameters so that it complies with constraints both theoretical and experimental

### 4.1 Theoretical constraints

For models with a scalar content larger than the SM's, special attention needs to be focussed on the possibility of the scalar potential becoming unbounded-from-below – meaning, tending to minus infinity for some direction along which the fields are assuming arbitrarily large values. This imposes constraints on the model's scalar quartic couplings, as the quartic part of the potential clearly dominates over the quadratic (or even an eventual cubic) one when the scalar fields tend to infinity. This is already a concern for the SM – it is the reason why the SM Higgs quartic coupling  $\lambda$  is taken positive. For the 2HDM generic conditions were found [31, 32] but for the 3HDM there is no such generic prescription upon which one might fall. Still, some *necessary* conditions are easy to find. Analysing the shape of the scalar potential of eq. (18), we see that if one takes each of the doublets  $\phi_i$  to infinity separately, the potential will tend to  $-\infty$  unless

$$\lambda_1 > 0 , \quad \lambda_2 > 0 , \quad \lambda_3 > 0. \quad (56)$$

Likewise, following a procedure similar to the one used in the 2HDM [15], if one takes two doublets  $(i, j)$  to infinity but such that  $\phi_i^\dagger \phi_j = 0$  (which is easily accomplishable, if for one doublet the upper components are

zero and for the other one the lower components vanish) one obtains a positive value of the potential for any value of the fields if

$$\lambda_4 > -2\sqrt{\lambda_1\lambda_2} , \quad \lambda_5 > -2\sqrt{\lambda_1\lambda_3} , \quad \lambda_6 > -2\sqrt{\lambda_2\lambda_3} . \quad (57)$$

We can also adapt the bounded-from-below necessary conditions from ref. [40] (their expressions 21–24), being careful with the fact that the potential of that work is different from ours (ours has a more restrictive symmetry, and therefore less quartic couplings). This translates into a generalisation of the above conditions, which become

$$\lambda_4 > -2\sqrt{\lambda_1\lambda_2} - \min(0, \lambda_7) , \quad \lambda_5 > -2\sqrt{\lambda_1\lambda_3} - \min(0, \lambda_8 - 2|\lambda_{10}|) , \quad \lambda_6 > -2\sqrt{\lambda_2\lambda_3} - \min(0, \lambda_9) . \quad (58)$$

Ultimately, these necessary conditions eliminate a great deal of parameter space, and though they are not *sufficient* ones, they should cover most of the parameter space leading to an unbounded-from-below potential.

Another strong constraint on the quartic couplings of potential is the requirement that the theory be unitary. For the SM this implied an upper bound on the mass of the Higgs boson [41, 42], and similar studies have been applied to the 2HDM (general unitarity conditions are presented in [34]) and other models with higher scalar content. Essentially, the method consists in computing all scalar-scalar  $J = 0$  scattering amplitudes (usually denoted  $a_0$ ) and requiring that they respect unitarity in the high energy regime. This translates into an upper bound on those amplitudes,  $|a_0| < 1/2$ . Theories with multi-scalars complicate the calculation somewhat since many such scattering amplitudes occur, and bounds must be imposed upon eigenvalues of the S-matrix. Again, the work of [40] is a precious help for our purposes: those authors deduced the general unitarity bounds for a 3HDM with a  $Z_2 \times Z_2$  model, of which our  $U(1) \times Z_2$  symmetry is a special case – since our model has a larger symmetry, it has less parameters than that of [40] and we can read off from their expressions 91–102 the unitarity constraints imposed upon the quartic couplings. **PLEASE EXPLAIN HERE WHAT WE DO REGARDING UNITARITY CONSTRAINTS IN SARAH, SPHENO, ETC.**

Finally, a “standard” constraint on multiscalar models is to verify their compliance with electroweak precision bounds. Models with  $N$  Higgs doublets automatically satisfy  $\rho = 1$  at tree-level, meaning bounds on the oblique parameter  $S$  will be easily satisfied – but that is no longer true for the  $T$  parameter, which must be computed for each model considered. Constraints on  $T$  typically force, for very high masses, degeneracies between the extra scalars of the model. The results from [40] are of no help to us in this case, as the expressions for the oblique parameters given there are only valid for a 3HDM version of the inert model (where one of the doublets is vevless and naturally decouples from the gauge sector). Therefore we **PLEASE EXPLAIN HERE WHAT WE DO REGARDING ELECTROWEAK PRECISION CONSTRAINTS IN SARAH, SPHENO, ETC.**

## 4.2 Experimental constraints

Since the discovery of the Higgs boson in 2012 the LHC collaborations have been able to verify that its properties conform by and large to those expected for the SM Higgs. This means, in practical terms, that the couplings of the 125 GeV  $h$  state to electroweak gauge bosons and fermions in a BSM model cannot deviate too much from the corresponding SM couplings. A convenient way of parameterizing this is by introducing the  $\kappa$ -formalism, defining the dimensionless quantities

$$\kappa_X^2 = \frac{\Gamma^{BSM}(h \rightarrow X)}{\Gamma^{SM}(h \rightarrow X)} \quad (59)$$

through the decay amplitudes  $\Gamma$ , computed in some BSM model and in the SM, of the Higgs to a certain final state  $X$  (typically  $ZZ$ ,  $WW$ ,  $\tau\bar{\tau}$  and  $b\bar{b}$ ). This definition means that exact SM behaviour would correspond to  $\kappa = 1$ , and LHC measurements [3, 4] already only allow a roughly 20% deviation from unity for the several  $\kappa$ 's. Requiring  $h$  to be SM-like naturally suppresses the couplings to gauge bosons of the heavier CP-even states  $H_1$  and  $H_2$  (these three states' gauge couplings obey a sum rule, due to gauge invariance). Since one of the most constraining channels in the search for heavier resonances at LHC is precisely via di-Z production, most constraints coming from those searches are automatically satisfied. There is however still an ample parameter space for which the heavier scalars also have suppressed production cross sections and could thus have avoided detection so far. To take into account the latest data from the LHC on the properties of the observed 125

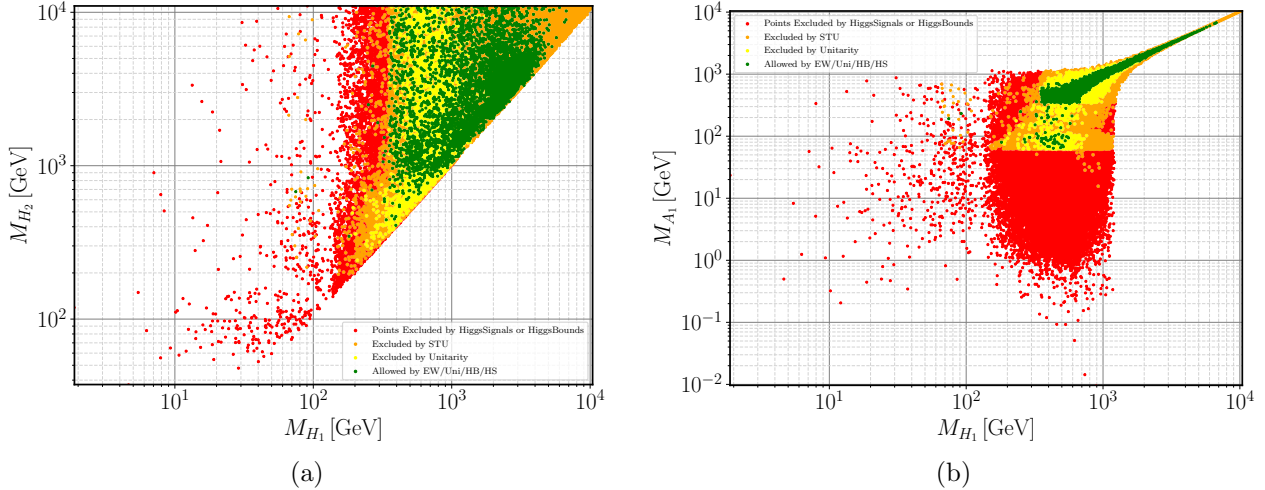


Figure 1: Scatter plots of parameter space allowed under several cuts imposed on the BGL-like 3HDM. In (a) we plot the masses of the two heavier CP-even scalars  $H_2$  and  $H_1$ ; in (b) we show the relation between the lightest (non- $h$ ) of the CP-even and pseudoscalar particles. Red points failed HS and HB tests; blue points failed HS tests; yellow points violate unitarity constraints; orange points only fail electroweak precision constraints, and green ones satisfy all restrictions. **(PF: MAYBE THE PLOTS END UP BEING TOO SMALL - MAKE IT INTO TWO FIGURES? OR PLACE PLOTS VERTICALLY?)**

GeV state we used `HiggsSignals` [43], and the searches (at LEP, Tevatron and LHC) for heavier CP-even and CP-odd scalars were taken into account through the use of `HiggsBounds` [44–46]. The measurements of the  $h_{125}$  properties at the LHC are included through the use of **PLEASE EXPLAIN HERE HOW THESE CODES ARE IMPLEMENTED IN OUR SCANS**.

As for the flavour sector, there are numerous observables that we need to check. The inverted procedure already ensures that our fit of the model has the correct quark masses and CKM matrix, but the presence of charged scalars, and neutral ones with FCNC interactions means that we must verify particularly sensitive quantities, such as the  $b \rightarrow s\gamma$  width, the neutral Kaons and  $B$ -meson mass differences and the CP-violating  $\epsilon_K$  phase, among others. To this end, **PLEASE EXPLAIN HERE WHAT WE DO REGARDING FLAVOUR CALCULATIONS - PRE-SPHENO, SPHENO, WILSON COEFFICIENTS, ETC.**

## 5 Results

**PF: HERE WE SHOULD BRIEFLY DESCRIBE THE FITTING PROCEDURE, AND THE RANGES ALLOWED. DISCUSS RESULTS OF SCAN IN TERMS OF ALLOWED PARAMETER SPACE; HOW MUCH POINTS SURVIVE DIFFERENT CUTS. DISCUSS FEATURES ALLOWED BY FINAL SCAN** In all that follows, we imposed *a priori* certain basic constraints: the correct electroweak symmetry breaking must occur, thus the doublets have vevs such that  $v_1^2 + v_2^2 + v_3^2 = (246 \text{ GeV})^2$ ; the lightest CP-even mass is 125 GeV; and the quartic couplings of the potential are chosen to obey the bounded-from-below necessary conditions described in section 4.1. Let us now investigate the effect that other cuts, both on the scalar and flavour sectors, have on the allowed parameter space of the model.

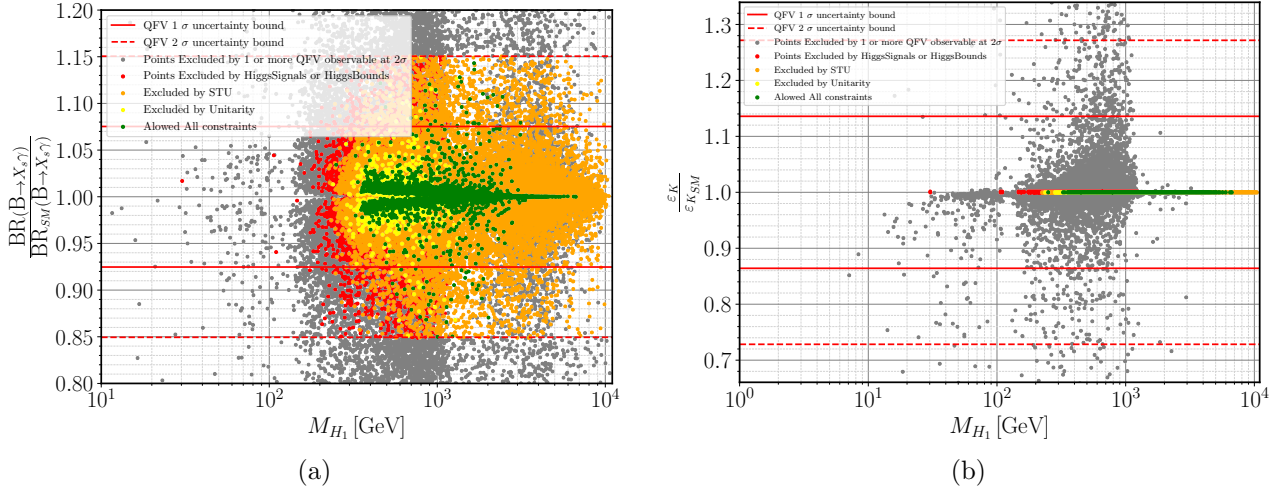


Figure 2: Scatter plots of parameter space allowed under several cuts imposed on the BGL-like 3HDM. In (a) we show the results for  $b \rightarrow s\gamma$  as a function of the  $H_1$  mass; in (b) we plot the results for  $\epsilon_K$  and a function of the  $H_1$  mass. Colour code as in fig. 1 and grey points are excluded, at the 2- $\sigma$  level, by at least one QFV observable.

## 5.1 Allowed parameter space

In fig. 1 we show the effect of non-flavour cuts in the allowed parameter space. Restrictions from LHC experiments, both in terms of measurement of the Higgs' properties or in searches for extra scalars, were taken into account using HiggsSignals (HS) and HiggsBounds (HB). Unitarity bounds on the model's quartic couplings are also imposed, as well as precision electroweak constraints via the S, T and U parameters. We see a close correlation between  $m_{A_1}$  and  $m_{H_1}$  for larger masses, stemming mostly from unitarity and electroweak precision constraints – the same tendency of near-degeneracy is observed in the mass spectrum of the 2HDM. Notice how our scan also included very low masses for the scalars, which are excluded by various experimental constraints from HiggsSignals.

In fig. 2 we show how some of the observables which depend on quark flavour violation (QFV) processes and might further constrain the parameter space which survives Higgs physics, unitarity and electroweak precision constraints. In fig. 2(a) we show how the ratio of the  $b \rightarrow s\gamma$  width computed in our BGL-like 3HDM to the expected SM value for that observable varies as a function of  $m_{H_1}$  – we observe a dispersion of values around the SM value, some of which beyond the 2- $\sigma$  uncertainties. As with most versions of the 2HDM, then, the  $b \rightarrow s\gamma$  constraint is a very important one, excluding many combinations of parameters otherwise perfectly acceptable. Not all flavour variables yield strong constraints, though – in fig. 2(b) we show the values obtained within our parameter scan for the Kaon system CP-violating  $\epsilon_K$  phase, and (please notice the vertical scale) can appreciate just how little variation around the SM value occurs, after all other QFV have been constrained to lie within a 2- $\sigma$  interval of their SM-expected values. This is clearly an indication that with our BGL-like 3HDM no substantial FCNC contributions to this observable will occur.

Having ascertained the relevance of the constraints imposed on the scalar sector, we now proceed with the results obtained for a different data sample from the one used in figs. 1 and 2, where only regions of parameter space where all bounds from boundedness from below, unitarity, electroweak precision variables, HiggsBounds and HiggsSignals are obeyed. We then analyse in detail what results for the flavour sector – since our model has tree-level FCNC, the inverted procedure described in section 3.3 does not guarantee a good fit in the model to quark flavour violating observables such as the mass differences for neutral  $K$ ,  $B_d$  and  $B_s$  mesons; the already mentioned  $\epsilon_K$  CP phase; decay widths such as  $B_0 \rightarrow \mu^+ \mu^-$ ; and many other such observables. Since the SM already does an extremely good job at describing the quark and lepton sector behaviour, we need to verify that new physics (NP) to those quantities do not ruin the existing agreement between theory and experiments. As

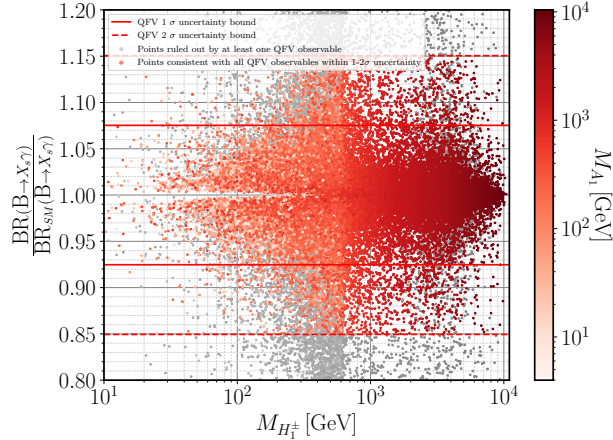


Figure 3:  $b \rightarrow s\gamma$  as a function of the  $H_1^\pm$  mass for the parameter space allowed under several cuts imposed on the BGL-like 3HDM. Red points (all tones of red) are those for which all QFV constraints are satisfied at most at  $2\sigma$  (many even at  $1\sigma$ ) level, grey points those for which at least one QFV observable is in disagreement with current measurements by more than  $2\sigma$ . The horizontal lines account for the current 1 and  $2\sigma$  uncertainties on  $b \rightarrow s\gamma$  measurements. The “temperature” gradient of colour shows where the lightest pseudoscalar contribute. (PF: IS IT NORMAL TO HAVE SUCH LOW CHARGED MASSES ALLOWED?)

we have already mentioned, our model being BGL-like ought to allow for an easy fit in the flavour sector, an assumption we now put to the test.

In fig. 3 we see how, after all Higgs sector constraints have been taken into account, automatic agreement with  $b \rightarrow s\gamma$  constraints is not automatic – in fact, we see (grey) points with larger than  $2\sigma$  disagreement occurring, and quite a few with disagreement with experimental  $b \rightarrow s\gamma$  values between 1 and  $2\sigma$ . These larger than  $1\sigma$  deviations are seen to occur mostly (though not exclusively) for lower masses of the lightest charged scalar,  $m_{H_1^\pm} \leq 700$  GeV. This is similar to what occurs for the Type II 2HDM [47]. Since in our model the down-type quark masses do not arise from a single  $\Gamma$  matrix, it is in fact natural that we find regions of parameter space for which observables such as  $b \rightarrow s\gamma$  behave in a similar manner to a Type II 2HDM. We however see that our 3HDM can fit this observable for much lower masses than 700 GeV, as occurs, for instance in a Type I 2HDM – again to be expected, certain regions of our parameter space should mimic well Type I behaviour. A similar phenomenon was observed for a 2HDM with tree-level FCNCs, see [9]. We further observe that the values of the  $b \rightarrow s\gamma$  width in our mode tend, for very large values of the lightest charged mass<sup>4</sup>, to the SM value. This is to be expected, as NP contributions to this observable depend in the inverse of the square of the extra scalars’ masses and are thus expected to tend to zero as those masses tend to infinity<sup>5</sup>.

In fig. 4, on the other hand, we observe how the inverted procedure we are using to fit the Yukawa sector yields excellent agreement with other QFV observables – there we plot the values of  $\epsilon_K$  as a function of the lightest charged mass, and see how close to the central value all the points we generated are. We see that this observable attains, in this model, values extremely close to the SM value, with deviations of the order of  $\sim 0.01\%$  – to put these results in context, the current experimental uncertainty on  $\epsilon_K$  stands at less than 0.5% of its central value. The minimal value of the charged mass that still reproduces the experimental value of  $\epsilon_K$  and satisfies all constraints is found to be  $\sim 150$  GeV.

<sup>4</sup>As we saw in fig. 1(b), theoretical and experimental constraints imposed upon the model force the extra scalars to have small mass splittings for large values of their mass. A value of  $m_{H_1^\pm}^\pm$  above 1 TeV thus corresponds to all extra scalar particles to have masses of the same order.

<sup>5</sup>In order to ensure consistency in the FLAVIO computation in both the SM and NP contributions (same choices of renormalization scales, particle masses, etc) we actually took  $BR_{SM}(B \rightarrow X_s\gamma)$  equal to the value of  $BR_{NP}(B \rightarrow X_s\gamma)$  obtained for the maximum scalar masses in our scan. A similar procedure was followed for other QFV computations.

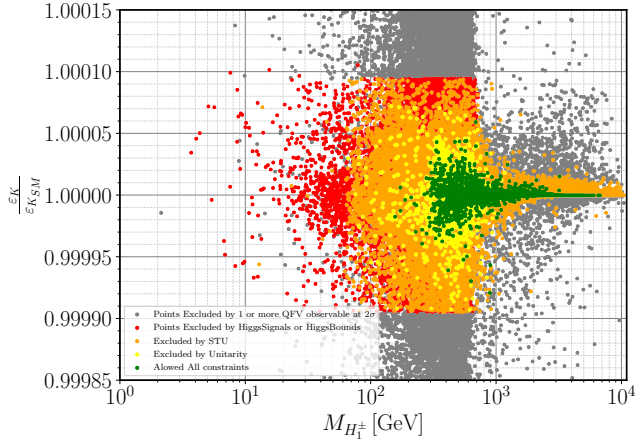


Figure 4:  $\epsilon_K$  as a function of the  $H_1^\pm$  mass for the parameter space allowed under several cuts imposed on the BGL-like 3HDM. Colour code as in fig. 3.

For completion, consider too the  $B$ -meson mass differences, observables which in the SM are generated by one-loop box diagrams, but which receive tree-level contributions in theories with scalars with FCNC interactions in the down sector. Again, and as expected, we see in figs. 5 and 6 that the values obtained in our BGL 3HDM for  $\Delta M_{B_s}$  and  $\Delta M_{B_d}$  tend to the SM value for large enough values of the extra scalars' masses. We also see that the fit procedure produces values of  $\Delta M_{B_d}$  extremely close to the SM value (even for lower masses), with larger dispersion found in  $\Delta M_{B_s}$ , although still easily fitting within a  $2\sigma$  variation. This is clearly due to the fact that we chose our structure for the Yukawa matrices (eqs. (52)) to single out the third generation – as expected through a BGL-like model, the FCNC interactions will be suppressed in a similar manner to the CKM matrix, and that explains how contributions to  $\Delta M_{B_d}$ , which involve a “jump” across two generations, are more suppressed than those contributions to  $\Delta M_{B_s}$ , for which scalars only “jump” one generation in their quark flavour-violating interactions.

Though we not show the results, we have analysed a wealth of other flavour observables, encountering  $1\sigma$  agreement with current experimental bounds for all of them. These included neutral Kaon mass differences and remaining QFV observables, neutral  $B$  mesons decays to muon and electron pairs and other leptonic sector measurements,  $Z \rightarrow b\bar{b}$  observables, etc.

**PF: DID WE CHECK Z TO BB? SHOULD WE MAKE A COMPLETE LIST HERE? SHOULD WE COMMENT UPON WHICH OBSERVABLES HAVE A TOUGHER TIME TO BE FITTED AT 1 SIGMA? THOSE WOULD BE B->S GAMMA AND WHAT ELSE?**

## 5.2 The Fine-Tuning Issue

The remarkable agreement found in the previous section for QFV observables, even when including the FCNC contributions from the extra scalars present in our model, needs to be analysed in depth. It can arise in several ways: for instance, if all extra scalar masses are very high, then the NP contributions take very small values and agreement with the SM value is easily found; another possibility is that the FCNC Yukawa interactions are *naturally* small, something which occurs in the 2HMD BGL model – their suppression by CKM matrix elements a consequence of the symmetry of the model – and which we claim also happens in the 3HDM version we are proposing; and finally, there is also the possibility of a fine tuning having occurred in the fitting procedure, “unnaturally” causing cancelations between different NP contributions. We will now see that this last possibility does not occur for our model.

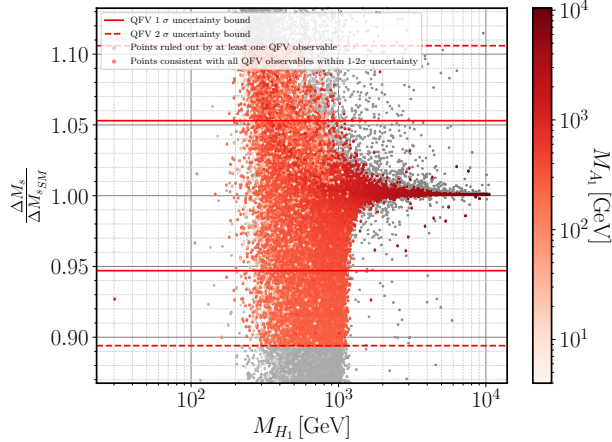


Figure 5:  $B_s$  mass difference as a function of the the CP-even  $H_1$  and pseudoscalar  $A_1$  masses. Colour code as in fig. 3.

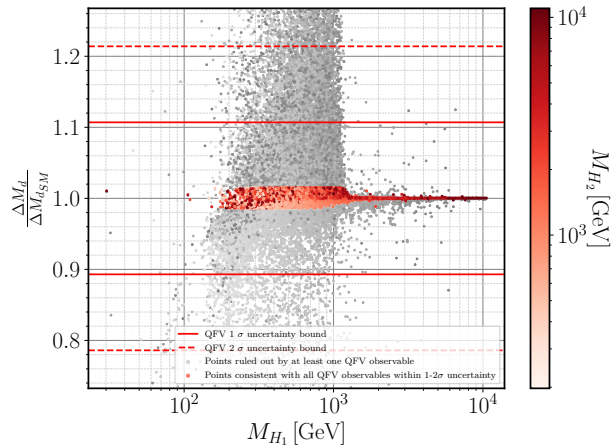


Figure 6:  $B_d$  mass difference as a function of heavier CP-even masses. Colour code as in fig. 3.

In order to see an example of such fine tuning, consider the Kaon system and observables such as the  $K^0 - \bar{K}^0$  mass difference, or the CP-violating phase  $\epsilon_K$ . The matrix element describing the transition  $\bar{K}^0 \rightarrow K^0$ ,  $M_{21}$ , receives contributions from the SM, via box diagrams, and from new physics (NP), through FCNC in the scalar sector:  $M_{21} = M_{21}^{\text{SM}} + M_{21}^{\text{NP}}$ . The NP terms arise from tree-level Feynman diagrams, and thus can in principle overwhelm the SM result – they originate in the tree-level exchange of CP-even and CP-odd scalars with FCNC interactions which, using the vacuum-insertion approximation (see refs. [6, 7, 9]) are found to be given by

$$M_{21}^{\text{K,NP}} = \frac{f_K^2 m_K}{96 v^2} \left\{ \frac{10m_K^2}{(m_s + m_d)^2} \left( \frac{F_{ds}^{dA_1}}{m_{A_1}^2} + \frac{F_{ds}^{dA_2}}{m_{A_2}^2} - \frac{F_{ds}^{dh}}{m_h^2} - \frac{F_{ds}^{dH_1}}{m_{H_1}^2} - \frac{F_{ds}^{dH_2}}{m_{H_2}^2} \right) + 4 \left[ 1 + \frac{6m_K^2}{(m_s + m_d)^2} \right] \left( \frac{\bar{F}_{ds}^{dA_1}}{m_{A_1}^2} + \frac{\bar{F}_{ds}^{dA_2}}{m_{A_2}^2} + \frac{\bar{F}_{ds}^{dh}}{m_h^2} + \frac{\bar{F}_{ds}^{dH_1}}{m_{H_1}^2} + \frac{\bar{F}_{ds}^{dH_2}}{m_{H_2}^2} \right) \right\}, \quad (60)$$

where  $f_K$  and  $m_K$  are the  $K$ -meson decay constant and mass, respectively, and the following combinations of FCNC couplings were defined, for each scalar/pseudoscalar  $X = \{h, H_1, H_2, A_1, A_2\}$ :

$$F_{ab}^{dX} = (N_{dX}^*)_{ab}^2 + (N_{dX})_{ba}^2,$$

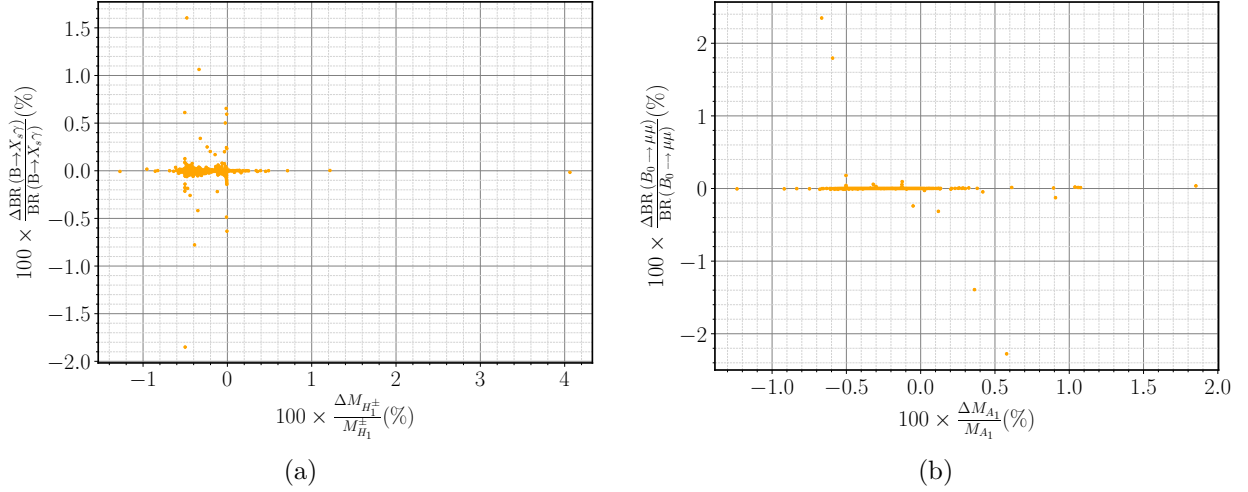


Figure 7: Percentage of variation of (a)  $b \rightarrow s\gamma$  branching ratio and (b) the  $B_0 \rightarrow \mu^+\mu^-$  decay width as a function of the percentage of variation in scalar masses. A set of parameters for which all constraints (experimental and theoretical) were satisfied, all scalar masses were smeared by less than 1% around their central values, keeping the Yukawa couplings and mixing angles fixed.

$$\bar{F}_{ab}^{dX} = (N_{dX}^*)_{ab} (N_{dX})_{ba}. \quad (61)$$

The matrices  $N_{dX}$  are obviously the Yukawa matrices for down-like quark interactions with each scalar  $X$ . We observe in eq. (60) that CP-even contributions tend to cancel CP-odd ones. This raises the possibility of being able to fit the Kaon observables if the CP-even and CP-odd terms, though large by themselves, cancel the the  $n^{th}$  decimal place, thus producing a result that, while in nominal agreement with experiments, is “unnatural”, and indeed such agreement might be spoiled by higher order corrections. Similar fine-tunings should be investigated in other observables, such as the  $B$  mesons mass difference, or semileptonic quantities such as the branching ratio of  $B_0 \rightarrow \mu^+\mu^-$ .

In order to investigate whether our results were or not fine-tuned, we began with one of the observables expected to be most sensitive to such variations ( $\epsilon_K$ ) and undertook the following procedure:

- Chose a combination of parameters for which all theoretical and experimental constraints are satisfied, and in particular the values predicted by the model for QFV observables are at most within  $2-\sigma$  of their experimental values.
- Fixed all the models’ parameters except for the soft breaking parameters, which were then smeared with a random variation of no more than 1% about their initial values. The scalar mass spectrum was recalculated and we chose those situations for which there were variations of less than 5% on all scalar masses.
- With the new value of the scalar masses (and all remaining mixing angles and Yukawa couplings equal to the values prior to the smearing described above) we recalculate the QFV observables and compare them with their initial values.

If there is a fine tuning in the calculation of  $\epsilon_K$ , for instance, a small oscillation in the masses, such as  $m_{A_1}$  or  $m_{H_1}$ , should provoke a much larger variation on the observable. We see the results of this procedure in fig. 7. We show the larger variations we observed, for the branching ratio for  $b \rightarrow s\gamma$  and  $B_0 \rightarrow \mu^+\mu^-$ . Similar variations were found for other observables, such as the meson mass differences  $\Delta M_d$  and  $\Delta M_s$  or the branching ratio for the decay  $B_s \rightarrow \mu^+\mu^-$ . Other observables had far smaller variations – for comparison, the absolute value of variations on  $\epsilon_K$ , for instance, were always seen to be less than 0.01%.

Thus we see that smearing the scalar masses by up to 4% around their central values (while keeping all mixing angles and Yukawa couplings the same) induces variations of less than 2.5 % on the value of QFV observables – we therefore conclude that in our BGL-like 3HDM the fits obtained to all observables are not the result of a fine-tuning, rather *the FCNC interactions of the model have been rendered naturally small by the symmetries of the model*, as in the 2HDM BGL.

### 5.3 LHC predictions

As we saw in the previous sections, the BGL-like 3HDM we are proposing can fit, despite tree-level FCNC interactions in the down sector, all current experimental constraints. Further, it can do so even with extra scalar masses below  $\sim 500$  GeV, which raises the tantalizing question: could such scalars have already been observed at LHC, or can current LHC data be used to exclude portions of the model’s parameter space? Further, what can one expect *vis-à-vis* future LHC sensitivity to potentially discover the extra scalars predicted in our model?

To begin with, we must recall that we have chosen to work in an exact alignment limit in this model. Thus, the CP-even scalars  $H_1$  and  $H_2$  have couplings to Z (and W) boson pairs exactly equal to zero. As such, experimental searches for extra scalar resonances decaying into Z or W boson pairs [48–50] are automatically satisfied in our parameter scan. Deviations from the alignment limit considered in more general scans might change somewhat that state of affairs, but given how SM-like the 125 GeV scalar at LHC is showing to be, the couplings of  $H_1$  and  $H_2$  to electroweak gauge bosons will always be heavily suppressed, so we will not consider non-alignment limit studies in the current work. However, the sum rule for scalar-gauge boson couplings – which in the exact alignment limit makes  $H_1$  and  $H_2$  gaugephobic – does not apply to Yukawa interactions. For instance, in the 2HDM or in SUSY models, interactions of the pseudoscalar  $A$  to fermion pairs may be enhanced (or suppressed) by factors of  $\tan\beta$ . A promising avenue for searches for additional scalars is therefore the di-tau channel, where current and future LHC sensitivities may well reveal their presence.

In fig. 8 we show the cross section for gluon-gluon production of a pseudoscalar (the lightest,  $A_1$ ) multiplied by its branching ratio into tau pairs, for a center-of-mass energy of 13 TeV. Cross sections for gluon-gluon fusion pseudoscalar production were obtained using **PF: WHAT EXACTLY? SARAH? SPHENO? DO THEY INTERFACE WITH SUSHI?**. The relevance of requiring agreement with QFV observables is emphasised in this plot, **(PF: THIS WAS THE OLD MEANING OF THE COLOUR CODE, IS IT STILL CORRECT?)** where grey represents points for which at least one such observable was found to deviate from its current experimental measurement by more than 2 standard deviations; blue showing points for which full  $1-\sigma$  agreements was found for all QFV observables. As was to be expected, the total signal strength for this channel diminishes as the pseudoscalar mass increases – see in particular the sharp drop-off around  $m_{A_1} \sim 375$  GeV, that is twice the top mass; for larger pseudoscalar masses, the decay channel  $A_1 \rightarrow t\bar{t}$  becomes kinematically possible and tends to reduce the branching ratio for  $A_1 \rightarrow \tau\bar{\tau}$ . Notice, however, that there are a number of points for lower masses which almost can be probed by current CMS bounds. Until the end of LHC’s run we can expect an increase in accumulated luminosity of at least a factor of 100 (**PF: IS THIS TRUE? I THINK SO!**), which would roughly lower the exclusion lines shown in fig. 8 by an order of magnitude. As such, we can expect measurements of this channels to at least exclude parts of the parameter space for  $m_{A_1} < 400$  GeV. In fact, we see in fig. 8 that the maximum of the signal strength occurs for  $m_{A_1} \simeq 350$  GeV, which is unsurprising, given that that roughly corresponds to twice the top mass – and it is well known that the gluon fusion cross section has a local maximum for a c.o.m. energy equal to twice the top mass, both for the production of a CP-even or a CP-odd scalar.

**PF: I AM NOT CERTAIN WHICH MECHANISM IS THE SECOND PRODUCTION CROSS SECTION; ALSO NEED TO UNIFORMISE PLOTS** The ditau channel is also appropriate in searches for a heavier CP-even state, as we see in fig. 9. As before, take notice of the expected sharp drop in the value of the signal rate for masses  $m_{H_1} > 2m_t$ . Both in direct gluon-gluon production of  $H_1$ , or in its associated production with a bottom quark pair, the obtained signal strength including the branching ratio for  $H_1 \rightarrow \tau\bar{\tau}$  is very close to the current CMS sensitivity for the lower mass region. Thus we see that our BGL-like 3HDM is close to being

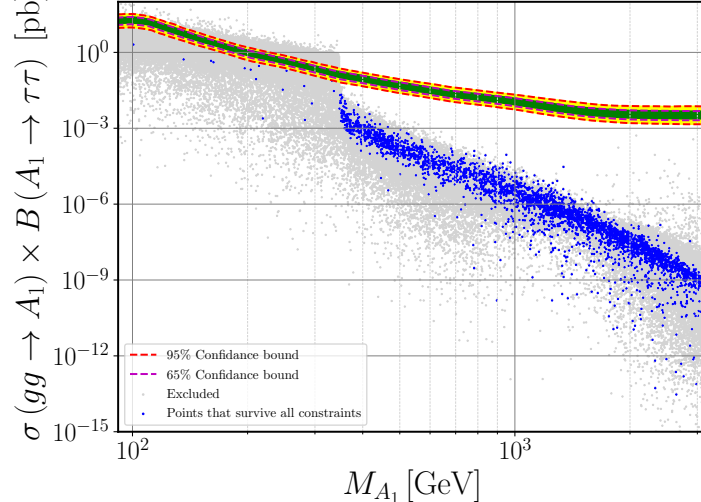


Figure 8: Gluon-gluon production cross section of a pseudoscalar at LHC at 13 TeV, times its branching ratio to  $\tau\bar{\tau}$  as a function of the lightest pseudoscalar mass  $m_{A_1}$ . Grey points represent sets of parameters excluded by not obeying at least one constraint (experimental or theoretical); blue points include agreement with all constraints and observables at least at the  $2-\sigma$  level. The 1- and  $2-\sigma$  observation limits from CMS for searches in this channel are also shown [?]. (PF: WHAT REFERENCES WERE USED IN THIS STUDY? LIKEWISE FOR ALL PLOTS WHICH QUOTE SEARCHES; IS THE DIFFERENCE BETWEEN GREY AND BLUE DUE ONLY TO QFV?)

probed by current LHC data, and before the end of the next run of data parts of its parameter space can be excluded by extra scalar searches. A parameter space which relaxes the condition of exact alignment – all the while maintaining full agreements with current LHC measurements of the properties of the lightest Higgs – would no doubt show a larger excluded region by the  $gg \rightarrow H_1 b\bar{b} \rightarrow \tau\bar{\tau} b\bar{b}$  channel.

Other search channels might also be considered (such as searches in decays to top pairs) but we relegate those analyses for a future paper where we will perform a more thorough scan of the model’s parameter space. Our main goal here is to prove, with a limited example, that the model is of interest for LHC searches.

## 6 Conclusions

Lighter than conventionally allowed nonstandard scalars which have potential for discovery at the colliders.

**Acknowledgements.** P.M.F. is supported by *Funda&atilde;o para a Ci&eacute;ncia e a Tecnologia* (FCT) through contracts CERN/FIS-PAR/0014/2019, UIDB/00618/2020 and UIDP/00618/2020 and by HARMONIA project’s contract UMO-2015/18/M/ST2/00518.

## References

- [1] **ATLAS** Collaboration, G. Aad et al., *Observation of a new particle in the search for the Standard Model Higgs boson with the ATLAS detector at the LHC*, *Phys. Lett. B* **716** (2012) 1–29, [[arXiv:1207.7214](https://arxiv.org/abs/1207.7214)].

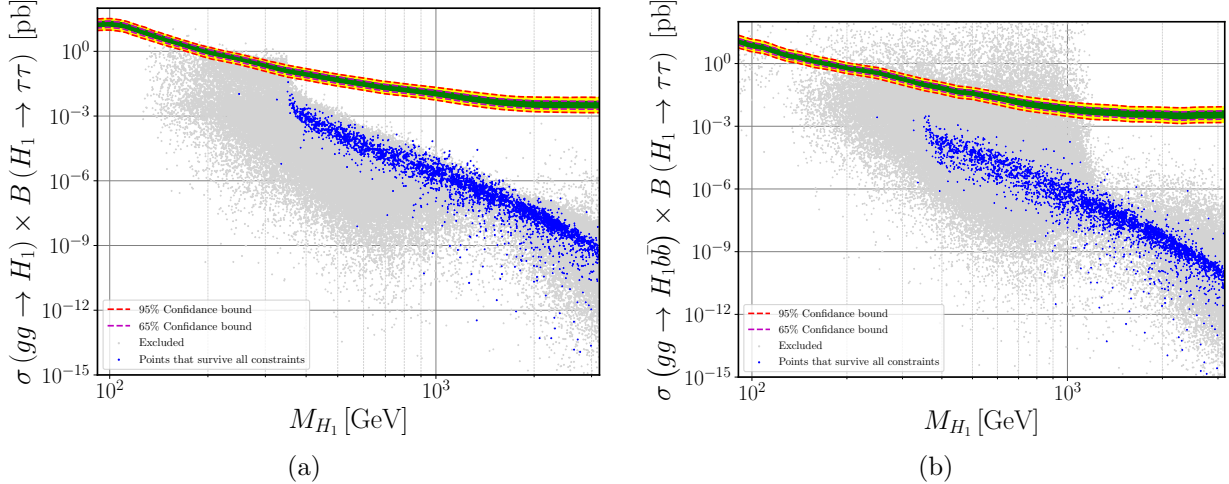


Figure 9: Signal strength for gluon-gluon production of a CP-even scalar (a) times its branching ratio to  $\tau\bar{\tau}$  (b) with associated production of a  $b$  quark pair and times its branching ratio to  $\tau\bar{\tau}$ , as a function of the lightest CP-even mass,  $m_{H_1}$ . Colour code as in fig. 8.

- [2] CMS Collaboration, S. Chatrchyan et al., *Observation of a new boson at a mass of 125 GeV with the CMS experiment at the LHC*, *Phys. Lett. B* **716** (2012) 30–61, [[arXiv:1207.7235](#)].
- [3] ATLAS, CMS Collaboration, G. Aad et al., *Combined Measurement of the Higgs Boson Mass in pp Collisions at  $\sqrt{s} = 7$  and 8 TeV with the ATLAS and CMS Experiments*, *Phys. Rev. Lett.* **114** (2015) 191803, [[arXiv:1503.07589](#)].
- [4] ATLAS, CMS Collaboration, G. Aad et al., *Measurements of the Higgs boson production and decay rates and constraints on its couplings from a combined ATLAS and CMS analysis of the LHC pp collision data at  $\sqrt{s} = 7$  and 8 TeV*, *JHEP* **08** (2016) 045, [[arXiv:1606.02266](#)].
- [5] T. D. Lee, *A Theory of Spontaneous T Violation*, *Phys. Rev. D* **8** (1973) 1226–1239.
- [6] G. C. Branco, L. Lavoura, and J. P. Silva, *CP Violation*, vol. 103. 1999.
- [7] P. Ferreira, L. Lavoura, J. P. Silva, and L. Lavoura, *A Soft origin for CKM-type CP violation*, *Phys. Lett. B* **704** (2011) 179–188, [[arXiv:1102.0784](#)].
- [8] M. Nebot and J. P. Silva, *Self-cancellation of a scalar in neutral meson mixing and implications for the LHC*, *Phys. Rev. D* **92** (2015), no. 8 085010, [[arXiv:1507.07941](#)].
- [9] P. Ferreira and L. Lavoura, *No strong CP violation up to the one-loop level in a two-Higgs-doublet model*, *Eur. Phys. J. C* **79** (2019), no. 7 552, [[arXiv:1904.08438](#)].
- [10] A. Pich and P. Tuzon, *Yukawa Alignment in the Two-Higgs-Doublet Model*, *Phys. Rev. D* **80** (2009) 091702, [[arXiv:0908.1554](#)].
- [11] M. Jung, A. Pich, and P. Tuzon, *Charged-Higgs phenomenology in the Aligned two-Higgs-doublet model*, *JHEP* **11** (2010) 003, [[arXiv:1006.0470](#)].
- [12] M. Jung, A. Pich, and P. Tuzon, *The  $B - \bar{B}$  Xs gamma Rate and CP Asymmetry within the Aligned Two-Higgs-Doublet Model*, *Phys. Rev. D* **83** (2011) 074011, [[arXiv:1011.5154](#)].
- [13] P. Ferreira, L. Lavoura, and J. P. Silva, *Renormalization-group constraints on Yukawa alignment in multi-Higgs-doublet models*, *Phys. Lett. B* **688** (2010) 341–344, [[arXiv:1001.2561](#)].

- [14] L. Lavoura, *Models of CP violation exclusively via neutral scalar exchange*, *Int. J. Mod. Phys. A* **9** (1994) 1873–1888.
- [15] G. Branco, W. Grimus, and L. Lavoura, *Relating the scalar flavor changing neutral couplings to the CKM matrix*, *Phys. Lett. B* **380** (1996) 119–126, [[hep-ph/9601383](#)].
- [16] F. Botella, G. Branco, A. Carmona, M. Nebot, L. Pedro, and M. Rebelo, *Physical Constraints on a Class of Two-Higgs Doublet Models with FCNC at tree level*, *JHEP* **07** (2014) 078, [[arXiv:1401.6147](#)].
- [17] F. Botella, G. Branco, M. Nebot, and M. Rebelo, *Flavour Changing Higgs Couplings in a Class of Two Higgs Doublet Models*, *Eur. Phys. J. C* **76** (2016), no. 3 161, [[arXiv:1508.05101](#)].
- [18] S. Weinberg, *Gauge Theory of CP Violation*, *Phys. Rev. Lett.* **37** (1976) 657.
- [19] P. Ferreira, I. P. Ivanov, E. Jimnez, R. Pasechnik, and H. Serdio, *CP4 miracle: shaping Yukawa sector with CP symmetry of order four*, *JHEP* **01** (2018) 065, [[arXiv:1711.02042](#)].
- [20] I. P. Ivanov, V. Keus, and E. Vdovin, *Abelian symmetries in multi-Higgs-doublet models*, *J. Phys. A* **45** (2012) 215201, [[arXiv:1112.1660](#)].
- [21] I. Ivanov and J. P. Silva, *CP-conserving multi-Higgs model with irremovable complex coefficients*, *Phys. Rev. D* **93** (2016), no. 9 095014, [[arXiv:1512.09276](#)].
- [22] A. Aranda, I. P. Ivanov, and E. Jimnez, *When the C in CP does not matter: anatomy of order-4 CP eigenstates and their Yukawa interactions*, *Phys. Rev. D* **95** (2017), no. 5 055010, [[arXiv:1608.08922](#)].
- [23] S. L. Glashow and S. Weinberg, *Natural Conservation Laws for Neutral Currents*, *Phys. Rev. D* **15** (1977) 1958.
- [24] E. A. Paschos, *Diagonal Neutral Currents*, *Phys. Rev. D* **15** (1977) 1966.
- [25] R. D. Peccei and H. R. Quinn, *CP Conservation in the Presence of Instantons*, *Phys. Rev. Lett.* **38** (1977) 1440–1443.
- [26] G. C. Branco, P. M. Ferreira, L. Lavoura, M. N. Rebelo, M. Sher, and J. P. Silva, *Theory and phenomenology of two-Higgs-doublet models*, *Phys. Rept.* **516** (2012) 1–102, [[arXiv:1106.0034](#)].
- [27] P. M. Ferreira, R. Santos, and A. Barroso, *Stability of the tree-level vacuum in two Higgs doublet models against charge or CP spontaneous violation*, *Phys. Lett. B* **603** (2004) 219–229, [[hep-ph/0406231](#)]. [Erratum: *Phys. Lett.B*629,114(2005)].
- [28] A. Barroso, P. M. Ferreira, and R. Santos, *Charge and CP symmetry breaking in two Higgs doublet models*, *Phys. Lett. B* **632** (2006) 684–687, [[hep-ph/0507224](#)].
- [29] A. Barroso, P. Ferreira, and R. Santos, *Neutral minima in two-Higgs doublet models*, *Phys. Lett. B* **652** (2007) 181–193, [[hep-ph/0702098](#)].
- [30] A. Barroso, P. Ferreira, R. Santos, and J. P. Silva, *Stability of the normal vacuum in multi-Higgs-doublet models*, *Phys. Rev. D* **74** (2006) 085016, [[hep-ph/0608282](#)].
- [31] I. P. Ivanov, *Minkowski space structure of the Higgs potential in 2HDM*, *Phys. Rev. D* **75** (2007) 035001, [[hep-ph/0609018](#)]. [Erratum: *Phys. Rev. D* **76**, 039902 (2007)].
- [32] I. P. Ivanov, *Minkowski space structure of the Higgs potential in 2HDM. II. Minima, symmetries, and topology*, *Phys. Rev. D* **77** (2008) 015017, [[arXiv:0710.3490](#)].
- [33] I. Ivanov and C. Nishi, *Symmetry breaking patterns in 3HDM*, *JHEP* **01** (2015) 021, [[arXiv:1410.6139](#)].
- [34] I. Ginzburg and I. Ivanov, *Tree-level unitarity constraints in the most general 2HDM*, *Phys. Rev. D* **72** (2005) 115010, [[hep-ph/0508020](#)].

- [35] N. G. Deshpande and E. Ma, *Pattern of Symmetry Breaking with Two Higgs Doublets*, *Phys.Rev.* **D18** (1978) 2574.
- [36] R. Barbieri, L. J. Hall, and V. S. Rychkov, *Improved naturalness with a heavy Higgs: An Alternative road to LHC physics*, *Phys.Rev.* **D74** (2006) 015007, [[hep-ph/0603188](#)].
- [37] Q.-H. Cao, E. Ma, and G. Rajasekaran, *Observing the Dark Scalar Doublet and its Impact on the Standard-Model Higgs Boson at Colliders*, *Phys.Rev.* **D76** (2007) 095011, [[arXiv:0708.2939](#)].
- [38] L. Lopez Honorez, E. Nezri, J. F. Oliver, and M. H. Tytgat, *The Inert Doublet Model: An Archetype for Dark Matter*, *JCAP* **0702** (2007) 028, [[hep-ph/0612275](#)].
- [39] D. Das and I. Saha, *Alignment limit in three Higgs-doublet models*, [arXiv:1904.03970](#).
- [40] S. Moretti and K. Yagyu, *Constraints on Parameter Space from Perturbative Unitarity in Models with Three Scalar Doublets*, *Phys. Rev. D* **91** (2015) 055022, [[arXiv:1501.06544](#)].
- [41] B. W. Lee, C. Quigg, and H. Thacker, *The Strength of Weak Interactions at Very High-Energies and the Higgs Boson Mass*, *Phys. Rev. Lett.* **38** (1977) 883–885.
- [42] B. W. Lee, C. Quigg, and H. Thacker, *Weak Interactions at Very High-Energies: The Role of the Higgs Boson Mass*, *Phys. Rev. D* **16** (1977) 1519.
- [43] P. Bechtle, S. Heinemeyer, O. Stål, T. Stefaniak, and G. Weiglein, *HiggsSignals: Confronting arbitrary Higgs sectors with measurements at the Tevatron and the LHC*, *Eur. Phys. J. C* **74** (2014), no. 2 2711, [[arXiv:1305.1933](#)].
- [44] P. Bechtle, O. Brein, S. Heinemeyer, G. Weiglein, and K. E. Williams, *HiggsBounds: Confronting Arbitrary Higgs Sectors with Exclusion Bounds from LEP and the Tevatron*, *Comput. Phys. Commun.* **181** (2010) 138–167, [[arXiv:0811.4169](#)].
- [45] P. Bechtle, O. Brein, S. Heinemeyer, G. Weiglein, and K. E. Williams, *HiggsBounds 2.0.0: Confronting Neutral and Charged Higgs Sector Predictions with Exclusion Bounds from LEP and the Tevatron*, *Comput. Phys. Commun.* **182** (2011) 2605–2631, [[arXiv:1102.1898](#)].
- [46] P. Bechtle, O. Brein, S. Heinemeyer, O. Stål, T. Stefaniak, G. Weiglein, and K. E. Williams, *HiggsBounds – 4: Improved Tests of Extended Higgs Sectors against Exclusion Bounds from LEP, the Tevatron and the LHC*, *Eur. Phys. J. C* **74** (2014), no. 3 2693, [[arXiv:1311.0055](#)].
- [47] A. Arbey, F. Mahmoudi, O. Stål, and T. Stefaniak, *Status of the Charged Higgs Boson in Two Higgs Doublet Models*, *Eur. Phys. J. C* **78** (2018), no. 3 182, [[arXiv:1706.07414](#)].
- [48] CMS Collaboration, A. M. Sirunyan et al., *Search for a new scalar resonance decaying to a pair of Z bosons in proton-proton collisions at  $\sqrt{s} = 13$  TeV*, *JHEP* **06** (2018) 127, [[arXiv:1804.01939](#)]. [Erratum: *JHEP* 03, 128 (2019)].
- [49] CMS Collaboration, A. M. Sirunyan et al., *Search for a heavy Higgs boson decaying to a pair of W bosons in proton-proton collisions at  $\sqrt{s} = 13$  TeV*, *JHEP* **03** (2020) 034, [[arXiv:1912.01594](#)].
- [50] ATLAS Collaboration, G. Aad et al., *Search for heavy diboson resonances in semileptonic final states in pp collisions at  $\sqrt{s} = 13$  TeV with the ATLAS detector*, [arXiv:2004.14636](#).